Electronic Supplementary Material (ESI) for Dalton Transactions.
This journal is © The Royal Society of Chemistry 2022

Electronic Supporting Information

Coordination Chemistry and Structural Rearrangements of the $Me_2PCH_2AlMe_2$ Ambiphilic Ligand

Katarina Paskaruk, David J. H. Emslie,* James F. Britten

Department of Chemistry, McMaster University, 1280 Main Street West, Hamilton, Ontario, L8S 4M1, Canada. Fax: (905)-522-2509; Tel: (905)-525-9140 x23307

E-mail: emslied@mcmaster.ca

Website: https://emsliegroup.mcmaster.ca/

Contents

NMR Spectra

NMR Spectra of [{κ²*P,P*-(Me₃AlCl)MeAl(CH₂PMe₂)₂}Rh(cod)] (1)

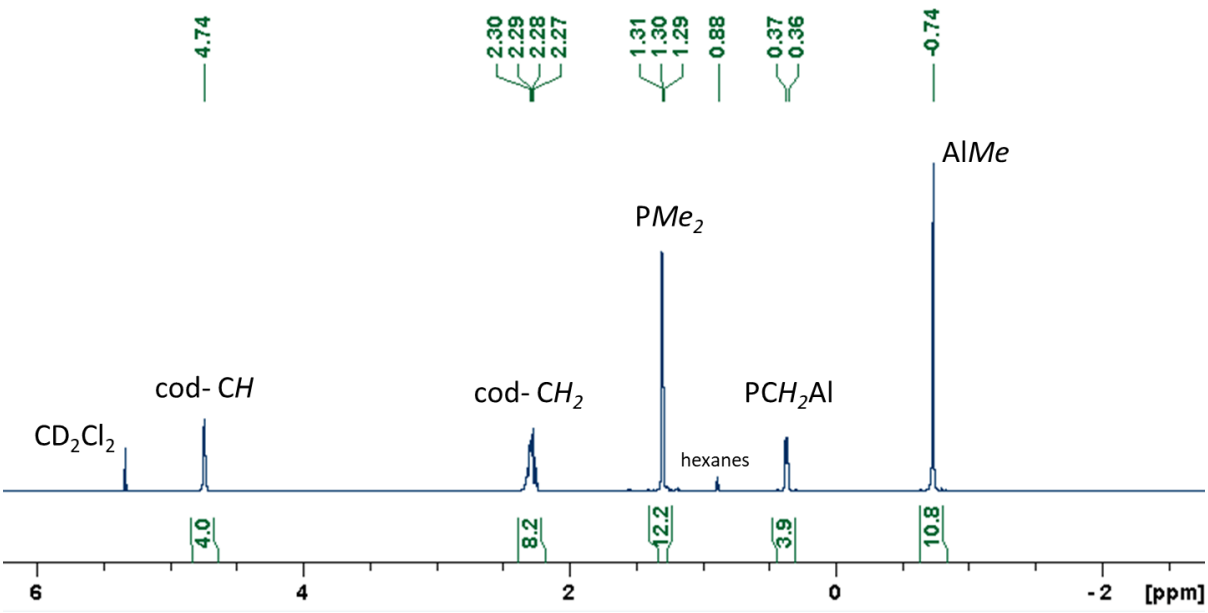

Figure S1. *^{1}H NMR Spectrum of [{κ²P,P-(Me₃AlCl)MeAl(CH₂PMe₂)₂}Rh(cod)] (**1**) in CD_2Cl_2 (600 MHz, 298K*). Note that the AlMe signal integrates to less than the expected 12H, indicating that some (<10%) $AlMe_3$ loss occurred during drying *in vacuo* (10 min at room temperature).

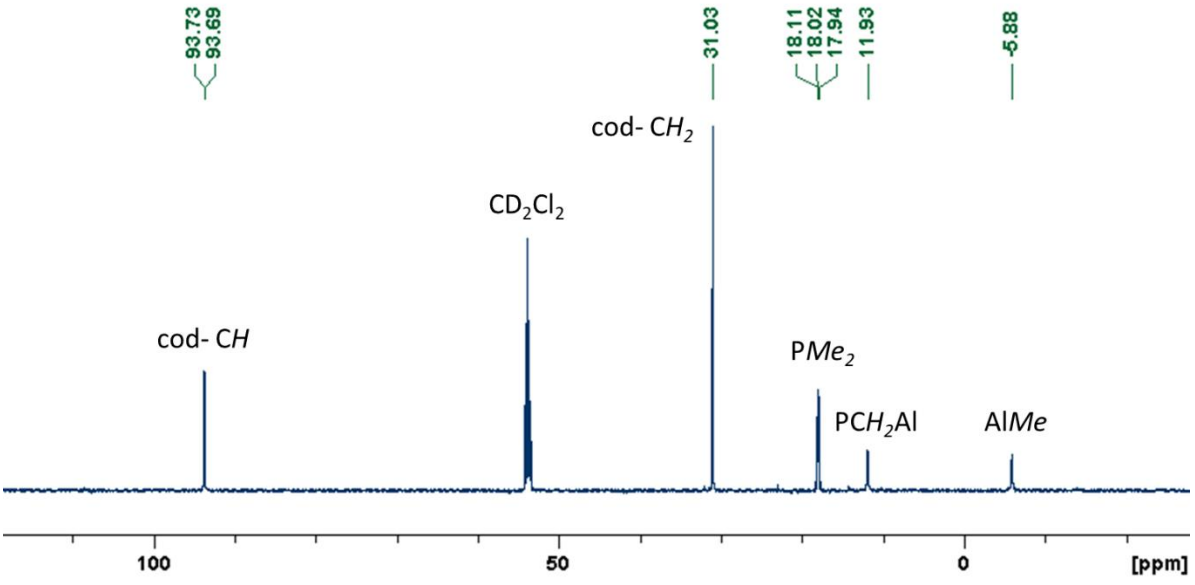

Figure S2. *$^{13}C\{^{1}H\}$ NMR Spectrum of [{κ²P,P-(Me₃AlCl)MeAl(CH₂PMe₂)₂}Rh(cod)] (**1**) in CD_2Cl_2 (150.9 MHz, 298K)*

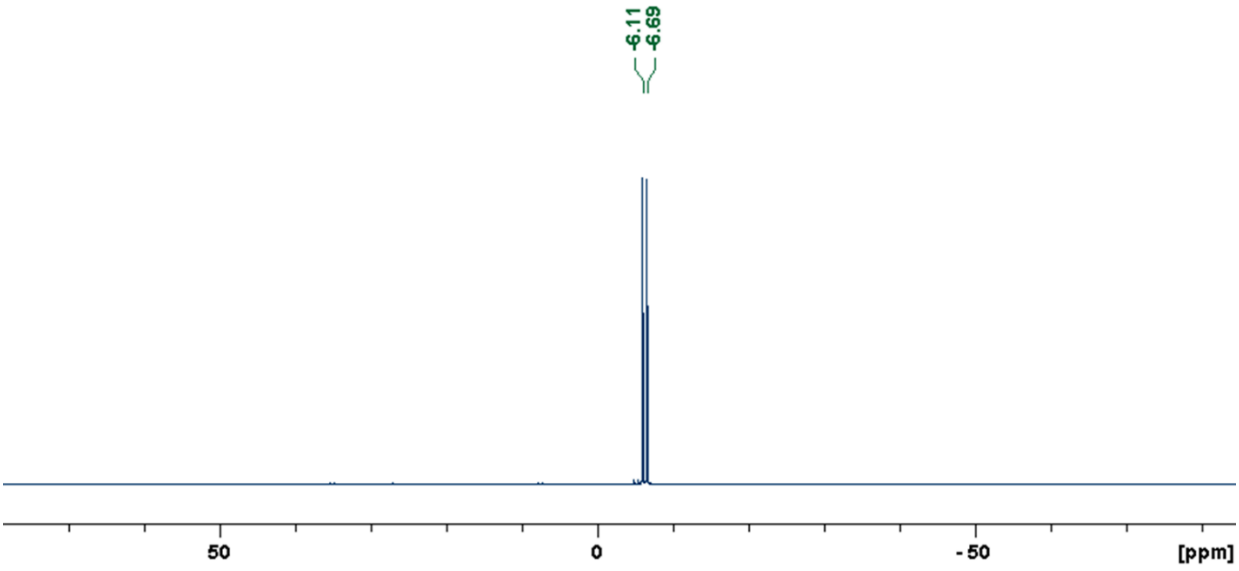

Figure S3. *$^{31}P\{^{1}H\}$ NMR Spectrum of [{κ²P,P-(Me₃AlCl)MeAl(CH₂PMe₂)₂}Rh(cod)] (**1**) in CD_2Cl_2 (242.9 MHz, 298K)*

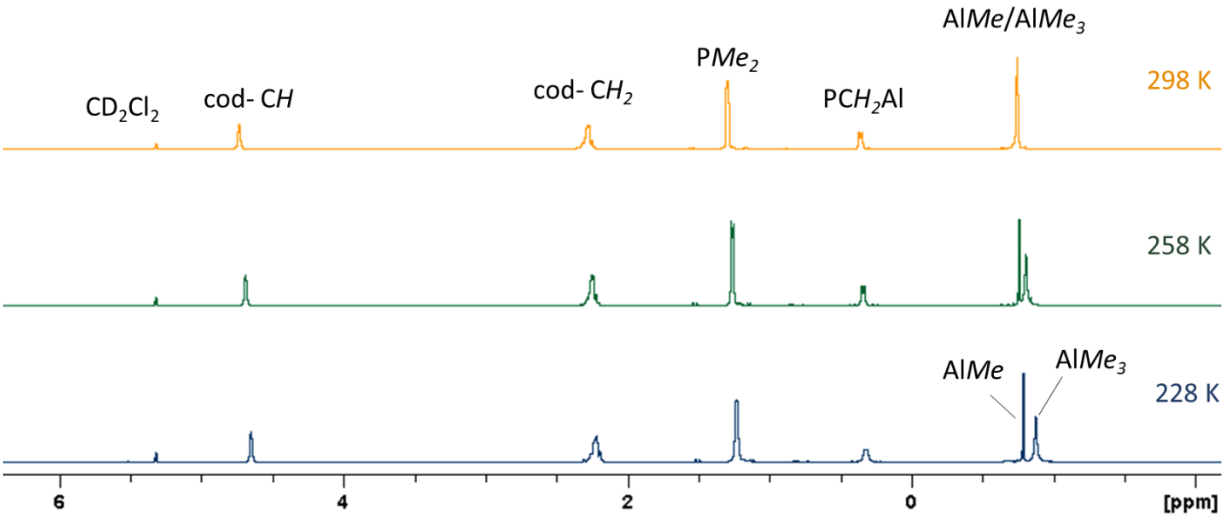

Figure S4. *^{1}H NMR Spectra of [{κ²P,P-(Me₃AlCl)MeAl(CH₂PMe₂)₂}Rh(cod)] (**1**) in CD_2Cl_2 (500 MHz) at 228, 258 and 298 K*

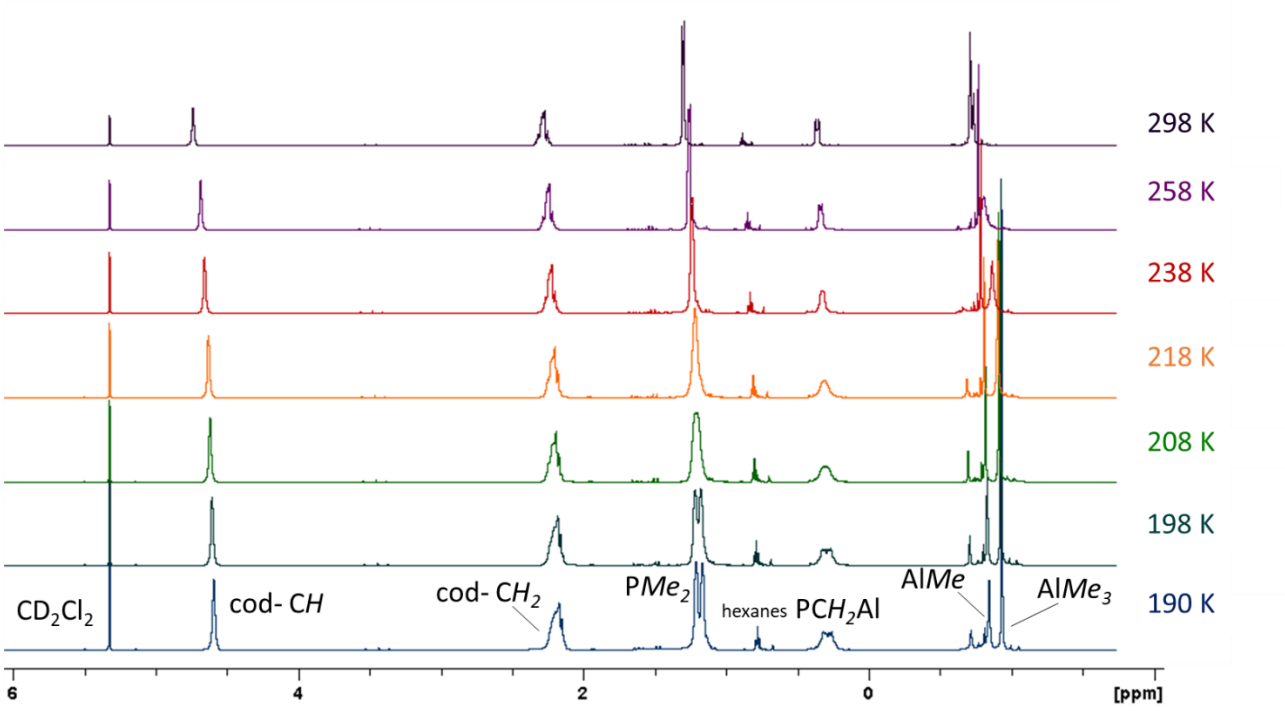

Figure S5. *^{1}H NMR Spectra of [{κ^{2}P,P-(Me$_3$AlCl)MeAl(CH$_2$PMe$_2$)$_2$}Rh(cod)] (**1**) in CD$_2$Cl$_2$ (500 MHz) between 295 and 190 K.*

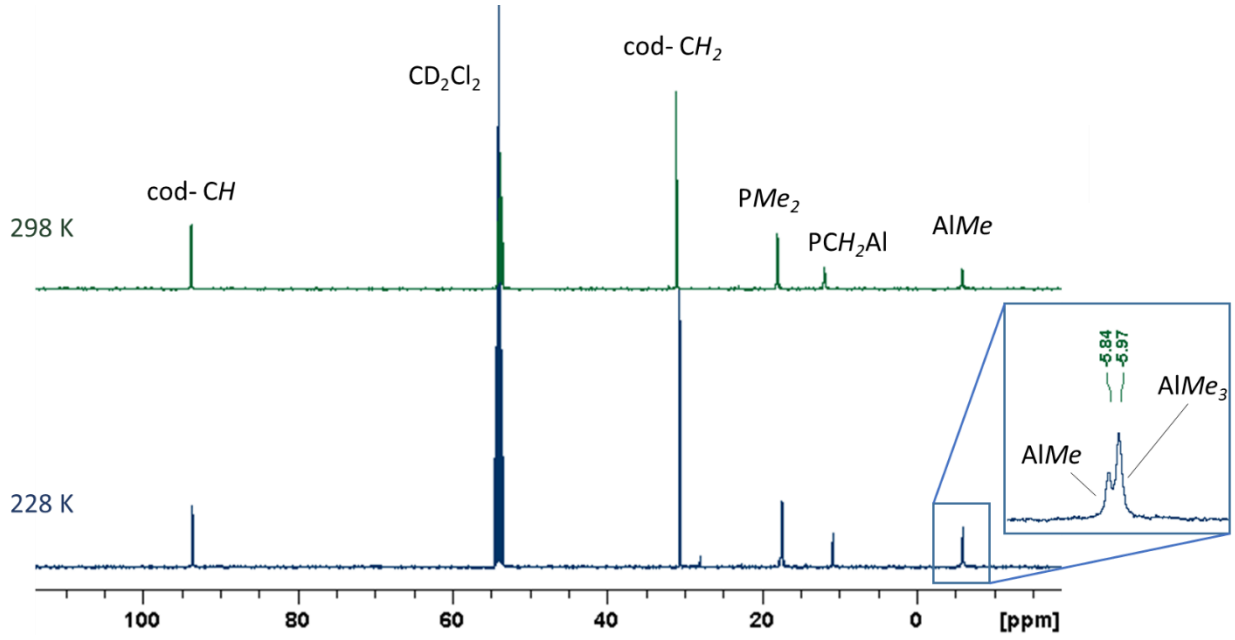

Figure S6. *^{13}C{^{1}H} NMR Spectra of [{κ^{2}P,P-(Me$_3$AlCl)MeAl(CH$_2$PMe$_2$)$_2$}Rh(cod)] (**1**) in CD$_2$Cl$_2$ (125.8 MHz) at 228 and 298K.*

NMR Spectra of [{κ²*P,P*-ClMeAl(CH₂PMe₂)₂}Rh(cod)] (2)

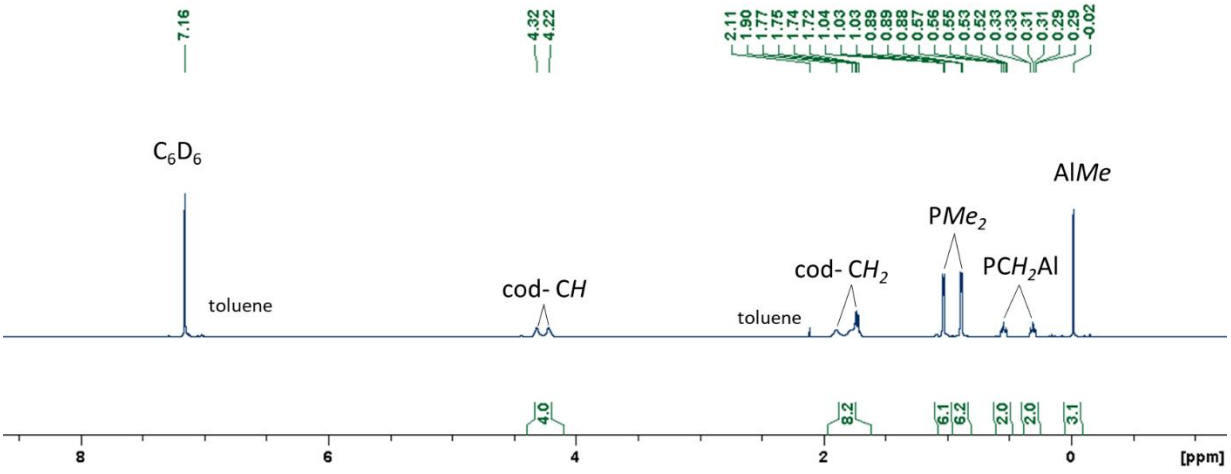

Figure S7. *^{1}H NMR Spectrum of [{κ²P,P-ClMeAl(CH₂PMe₂)₂}Rh(cod)] (**2**) in C_6D_6 (600 MHz, 298K) .*

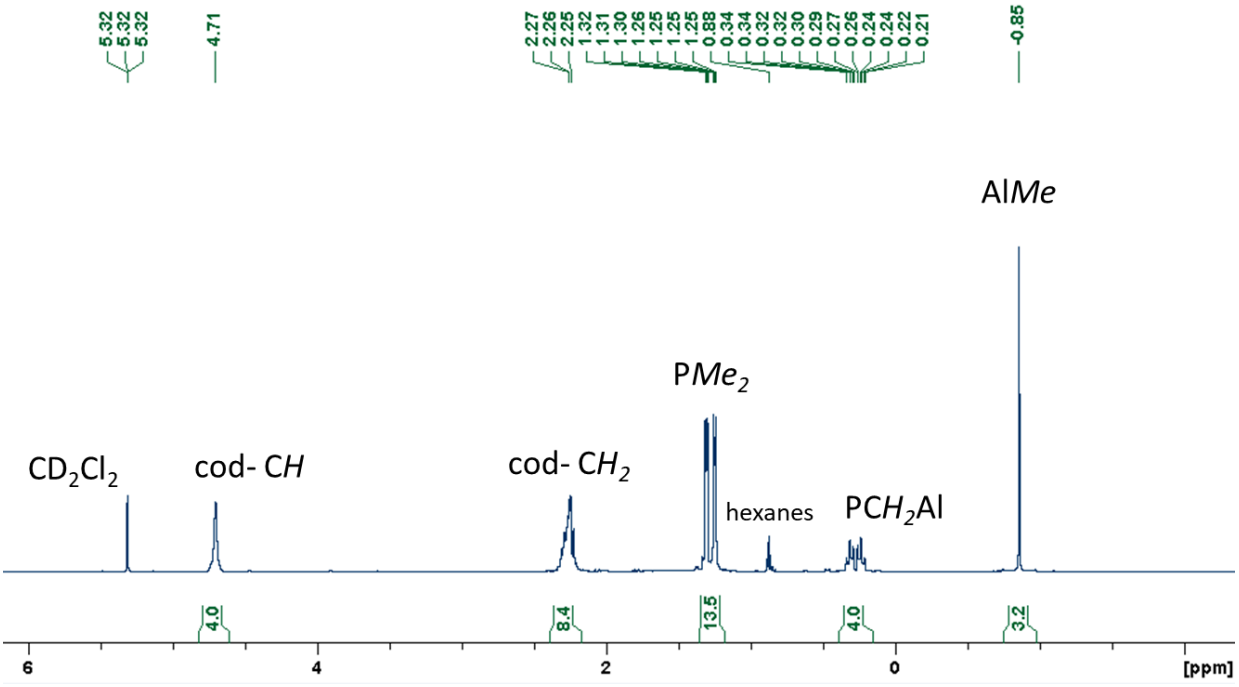

Figure S8. *^{1}H NMR Spectrum of [{κ²P,P-ClMeAl(CH₂PMe₂)₂}Rh(cod)] (**2**) in CD_2Cl_2 (500 MHz, 298K).*

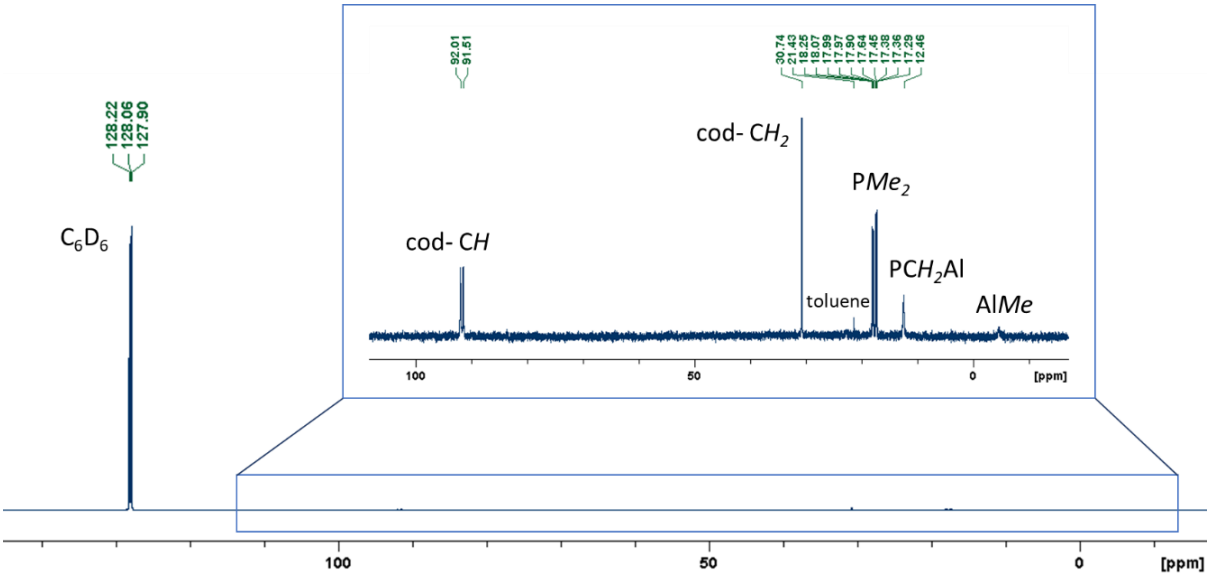

Figure S9. *$^{13}C\{^{1}H\}$ NMR Spectrum of [{κ²P,P-ClMeAl(CH₂PMe₂)₂}Rh(cod)] (**2**) in C_6D_6 (150.9 MHz, 298K).*

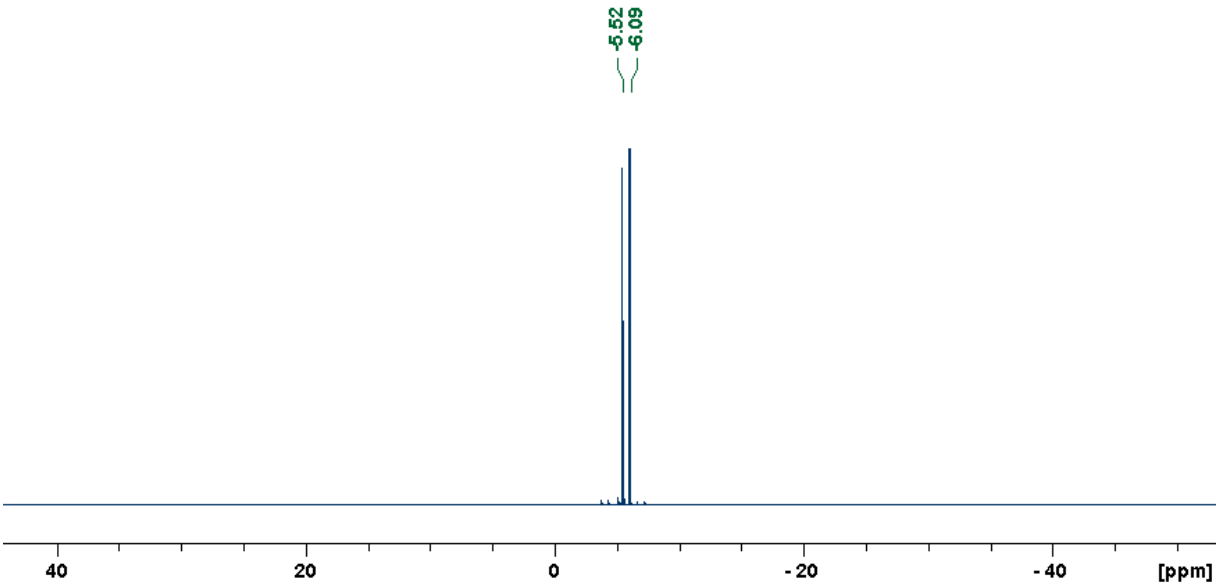

Figure S10. *$^{31}P\{^{1}H\}$ NMR Spectrum of [{κ²P,P-ClMeAl(CH₂PMe₂)₂}Rh(cod)] (**2**) in C_6D_6 (242.9 MHz, 298K).*

NMR Spectra of [Rh(cod)(μ-Cl)($Me_2PCH_2AlMe_2$)] (3) / [Rh(cod)(μ-Cl)($Me_2PCH_2AlClMe$)] (3A)

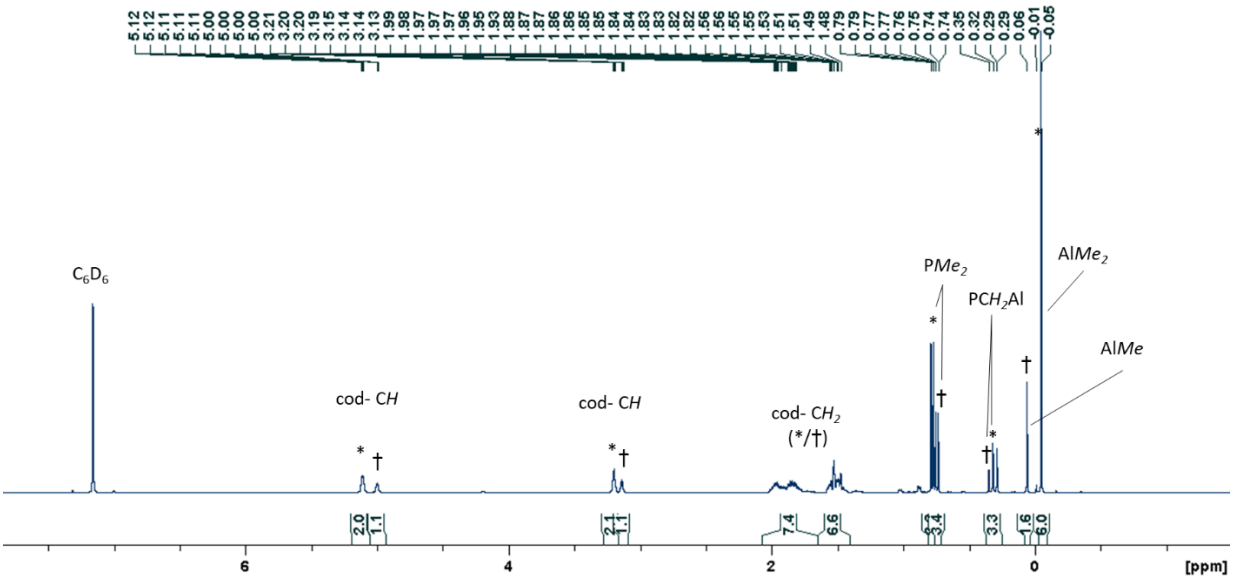

Figure S11. *^{1}H NMR Spectrum of [Rh(cod)(μ-Cl)($Me_2PCH_2AlMe_2$)] (**3**; *) / [Rh(cod)(μ-Cl)($Me_2PCH_2AlClMe$)] (**3A**; †) in C_6D_6 (500 MHz, 298 K), taken from single crystals of **3/3A** isolated from the 1:1 reaction of ($Me_2PCH_2AlMe_2$)$_2$ with [{RhCl(cod)}$_2$].*

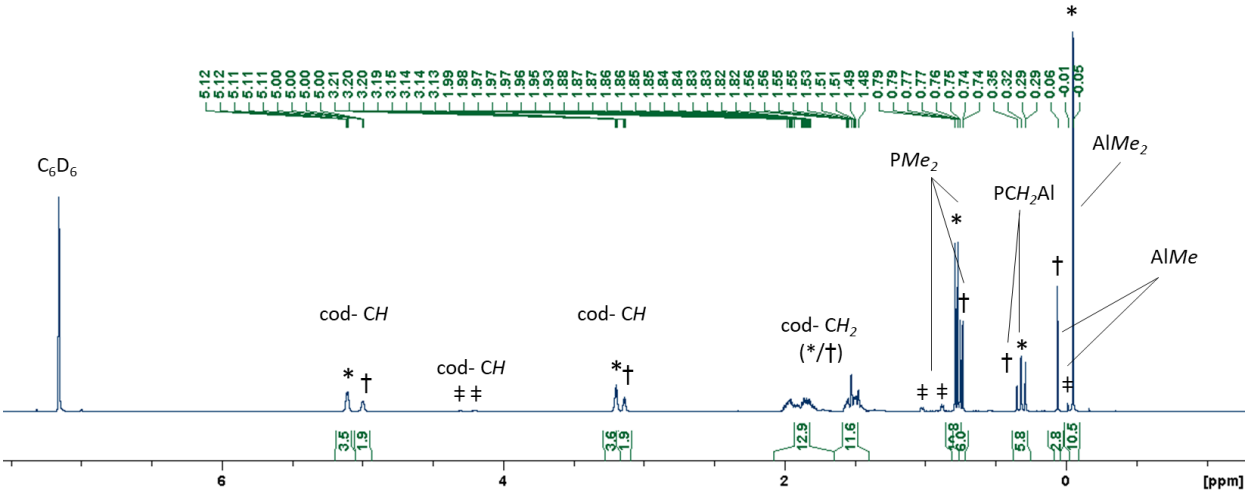

Figure S5. ^{1}H NMR Spectrum (C_6D_6, 500 MHz, 298 K) of the 1:1 reaction of ($Me_2PCH_2AlMe_2$)$_2$ with [{RhCl(cod)}$_2$], showing [Rh(cod)(μ-Cl)($Me_2PCH_2AlMe_2$)] (**3**; *) as the major product, accompanied by small amounts of [Rh(cod)(μ-Cl)($Me_2PCH_2AlClMe$)] (**3A**; †) and **2** (‡).

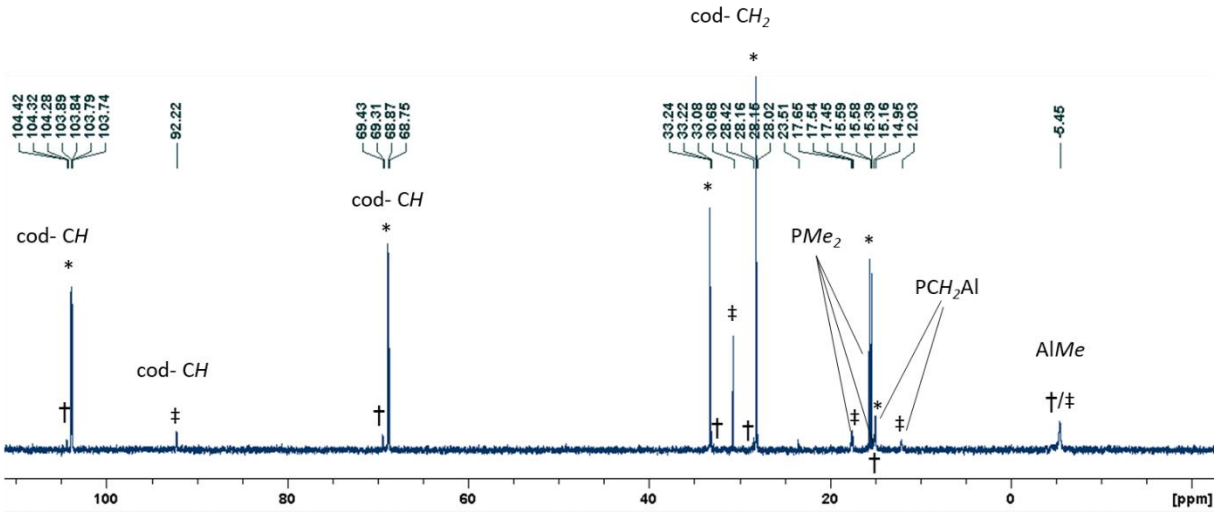

Figure S13. *$^{13}C\{^1H\}$ NMR Spectrum (C_6D_6, 125 MHz, 298 K) of the 1:1 reaction of $(Me_2PCH_2AlMe_2)_2$ with $[\{RhCl(cod)\}_2]$, showing $[Rh(cod)(\mu\text{-}Cl)(Me_2PCH_2AlMe_2)]$ (**3**; *) as the major product, accompanied by small amounts of $[Rh(cod)(\mu\text{-}Cl)(Me_2PCH_2AlClMe)]$ (**3A**; †) and **2** (‡).*

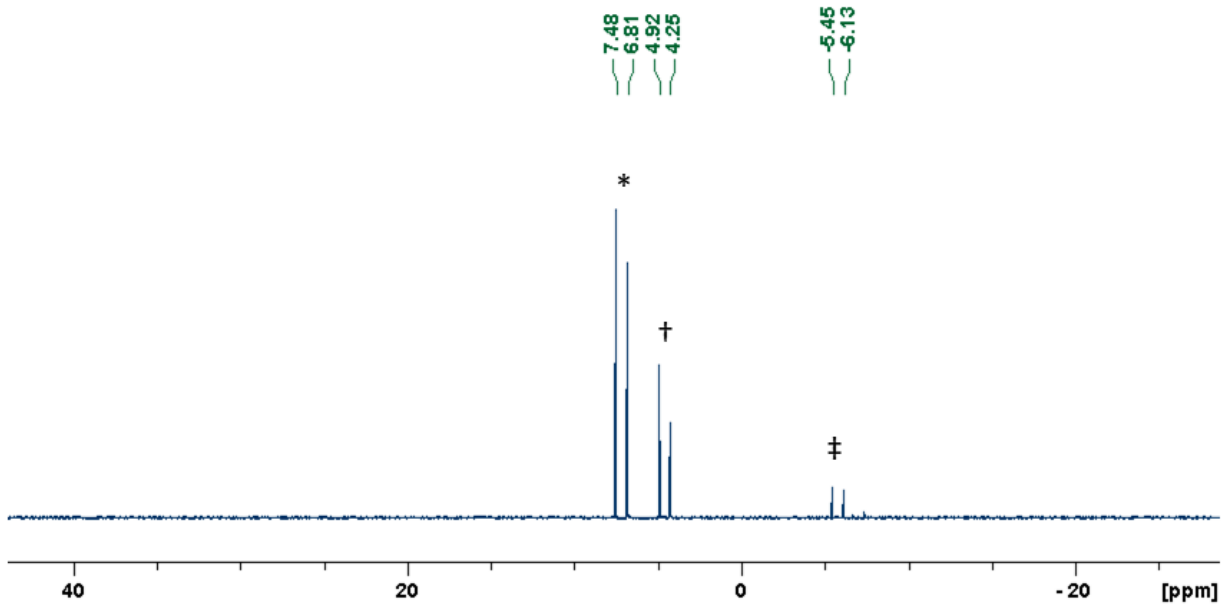

Figure S14. *$^{31}P\{H\}$ NMR Spectrum (C_6D_6, 202.5 MHz, 298 K) of the 1:1 reaction of $(Me_2PCH_2AlMe_2)_2$ with $[\{RhCl(cod)\}_2]$, showing $[Rh(cod)(\mu\text{-}Cl)(Me_2PCH_2AlMe_2)]$ (**3**; *) as the major product, accompanied by small amounts of $[Rh(cod)(\mu\text{-}Cl)(Me_2PCH_2AlClMe)]$ (**3A**; †) and **2** (‡).*

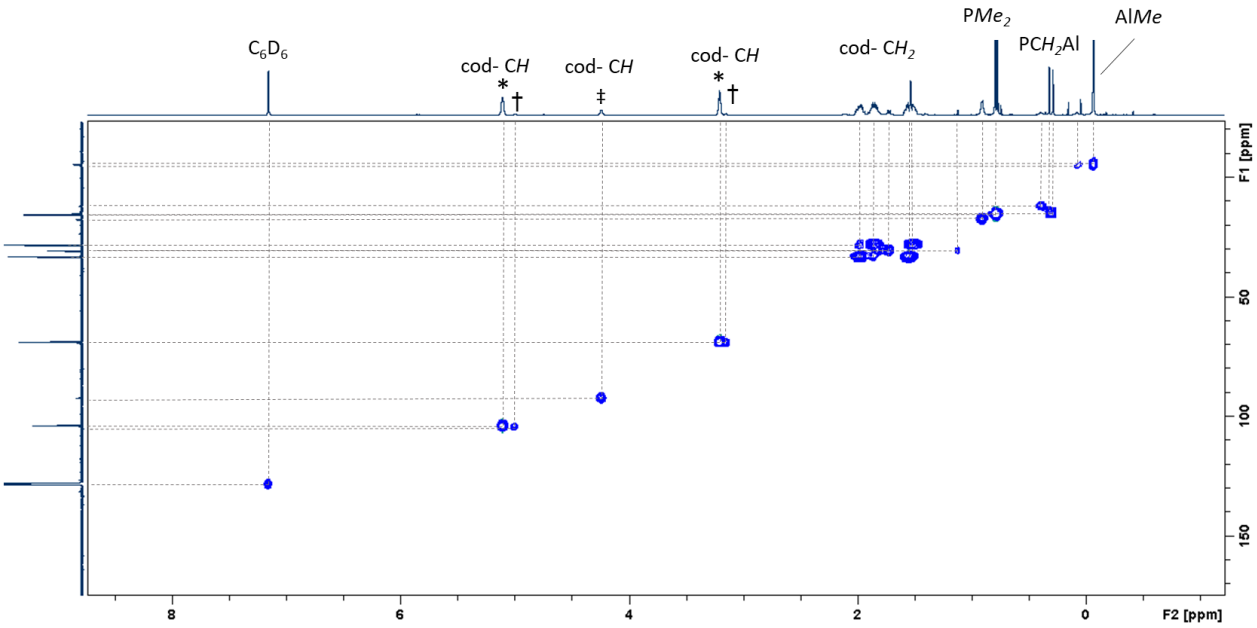

Figure S15. *2D ^{1}H-^{13}C HSQC NMR Spectrum (C_6D_6, 500/125 MHz, 298 K) of the 1:1 reaction of $(Me_2PCH_2AlMe_2)_2$ with $[\{RhCl(cod)\}_2]$, showing $[Rh(cod)(\mu\text{-}Cl)(Me_2PCH_2AlMe_2)]$ (**3**; *) as the major product, accompanied by small amounts of $[Rh(cod)(\mu\text{-}Cl)(Me_2PCH_2AlClMe)]$ (**3A**; †) and **2** (‡).*

NMR Spectra of $[\{Rh(\mu\text{-}CH_2PMe_2)(cod)\}_2]$ (4)

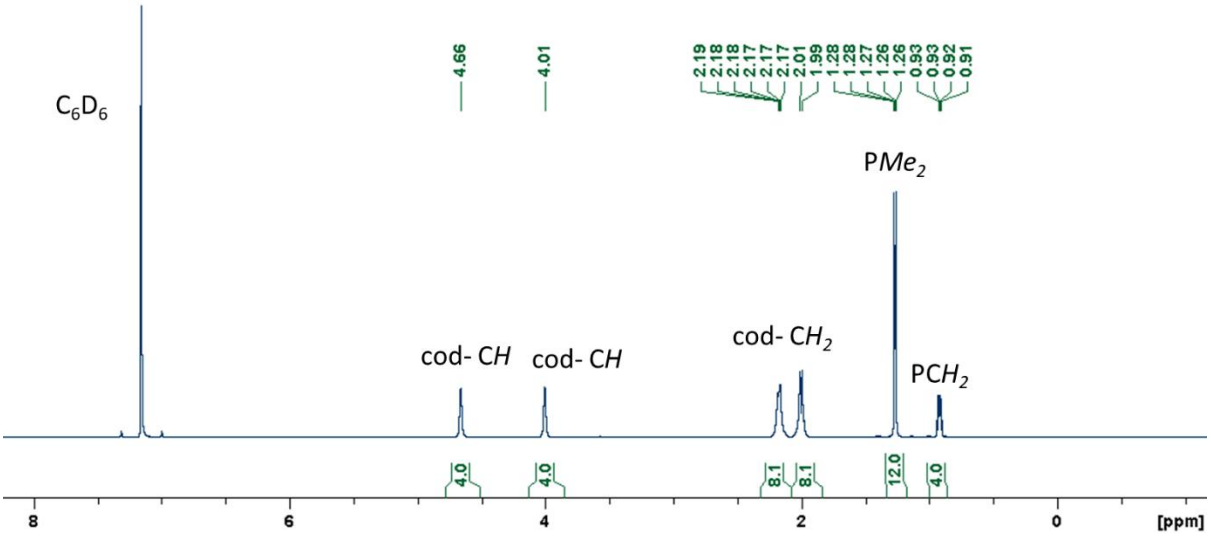

Figure S16. *^{1}H NMR Spectrum of $[\{Rh(\mu\text{-}CH_2PMe_2)(cod)\}_2]$ (**4**) in C_6D_6 (500 MHz, 298 K).*

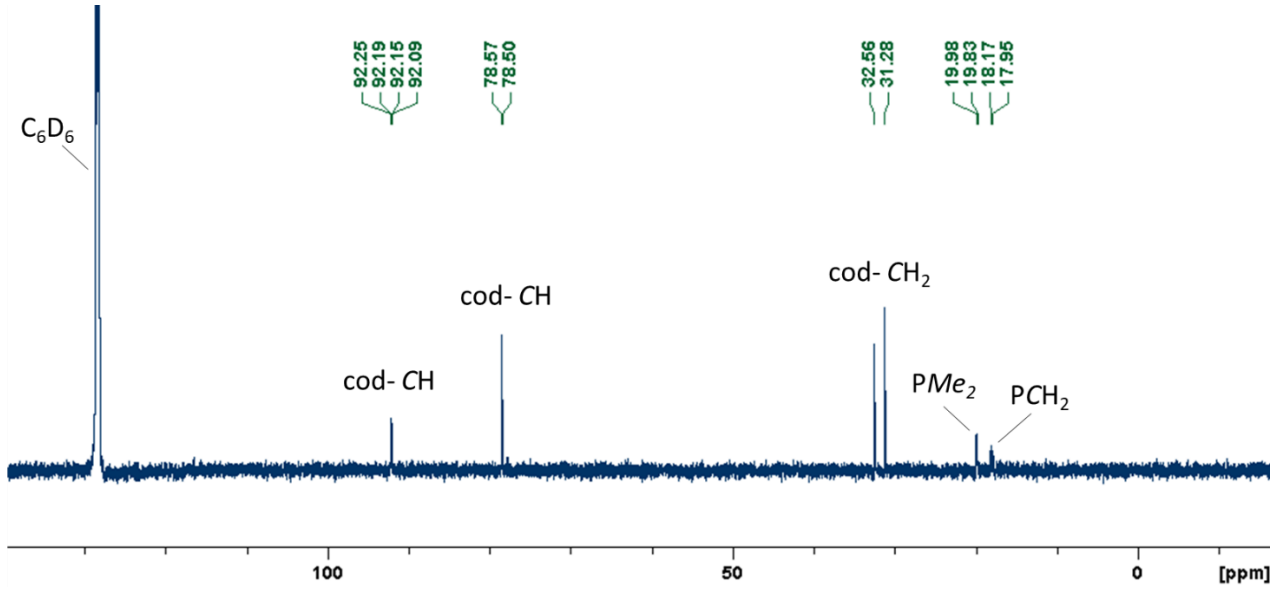

Figure S17. *$^{13}C\{^1H\}$ NMR Spectrum of [{Rh(μ-CH_2PMe_2)(cod)}$_2$] (**4**) in C_6D_6 (125.8 MHz, 298 K).*

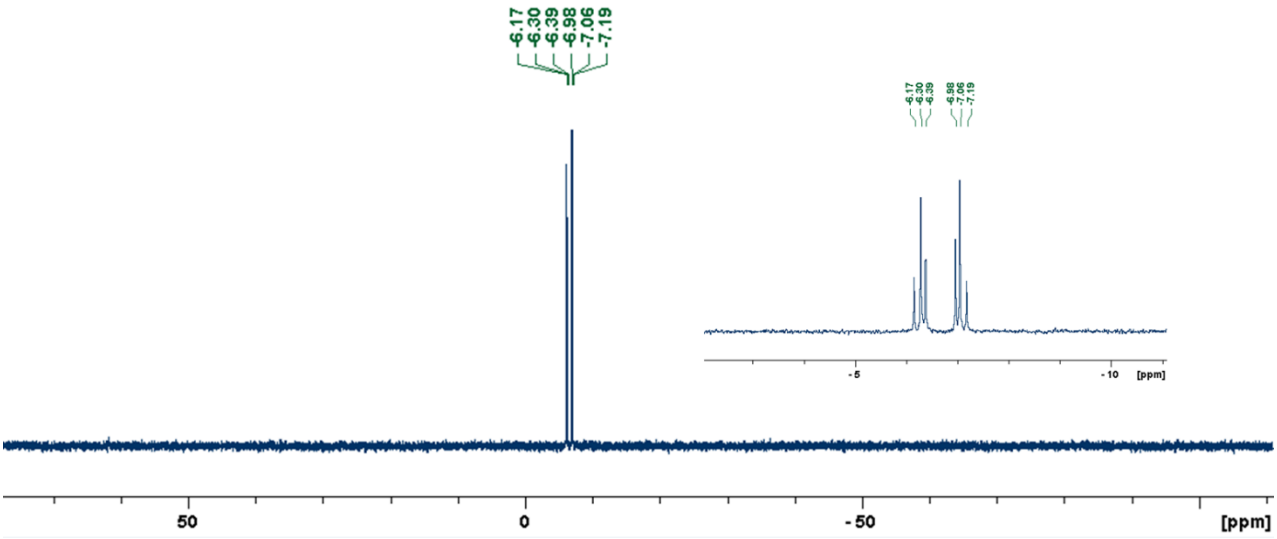

Figure S18. *$^{31}P\{^1H\}$ NMR Spectrum of [{Rh(μ-CH_2PMe_2)(cod)}$_2$] (**4**) in C_6D_6 (202.5 MHz, 298 K).*

NMR Spectra of [{κ²*P*,*P*-Cl₂Al(CH₂PMe₂)₂}Ir(cod)] (5)

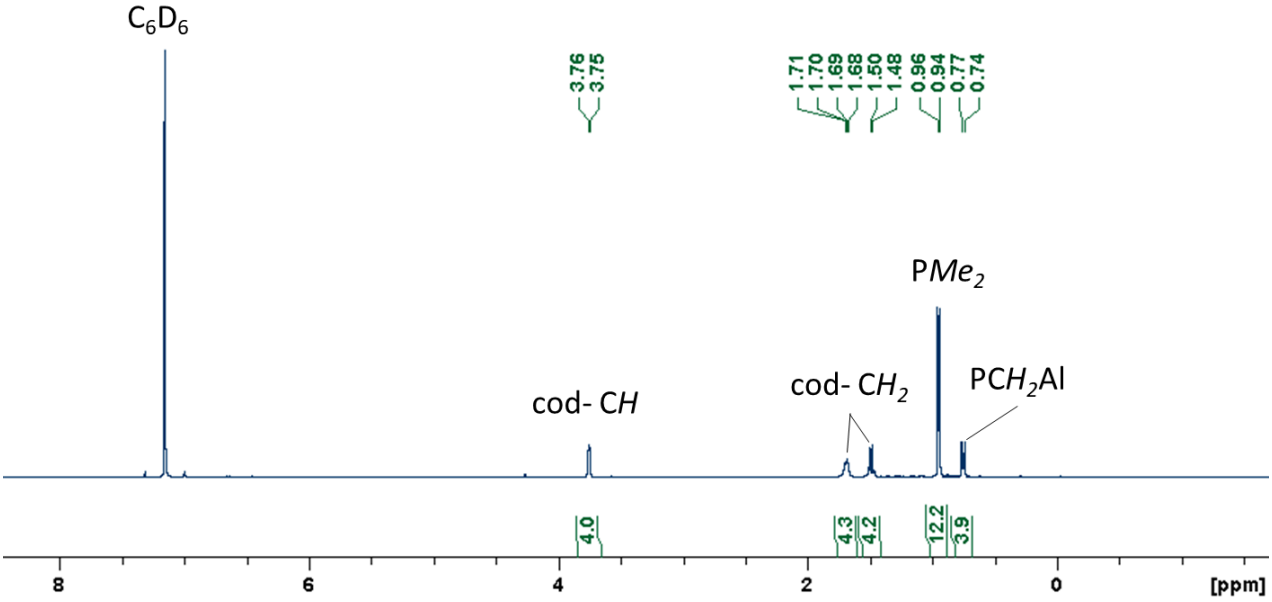

Figure S19. *^{1}H NMR Spectrum of [{κ²P,P-Cl₂Al(CH₂PMe₂)₂}Ir(cod)] (**5**) in C₆D₆ (500 MHz, 298 K).*

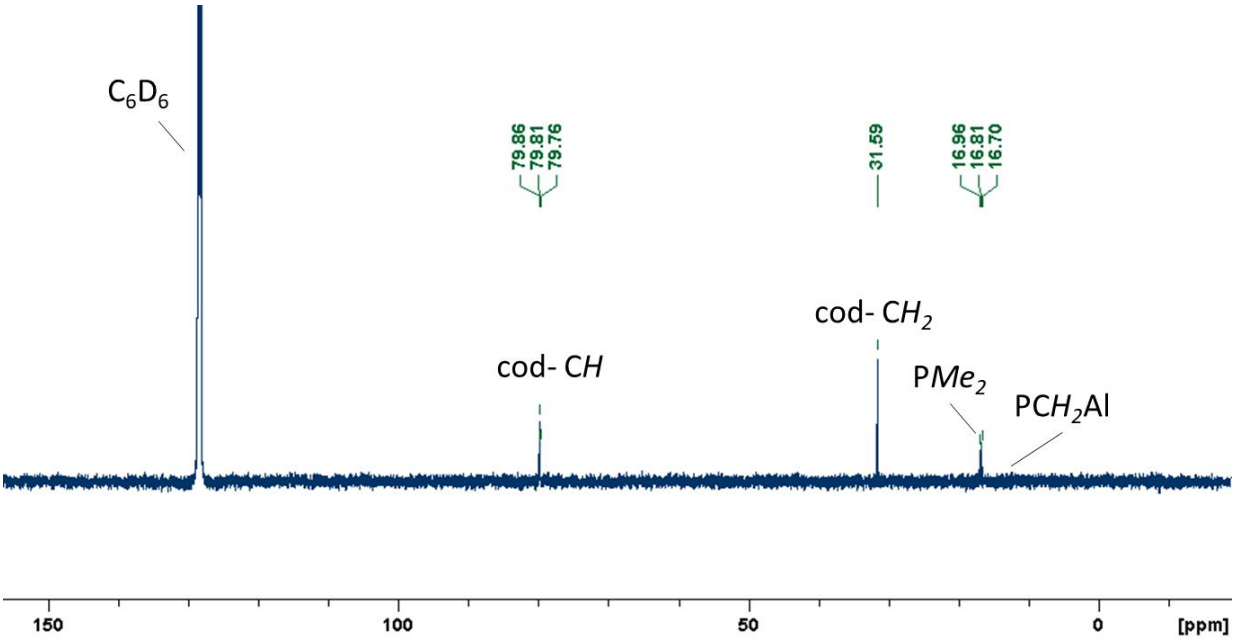

Figure S20. *^{13}C{^{1}H} NMR Spectrum of [{κ²P,P-Cl₂Al(CH₂PMe₂)₂}Ir(cod)] (**5**) in C₆D₆ (125.8 MHz, 298K).*

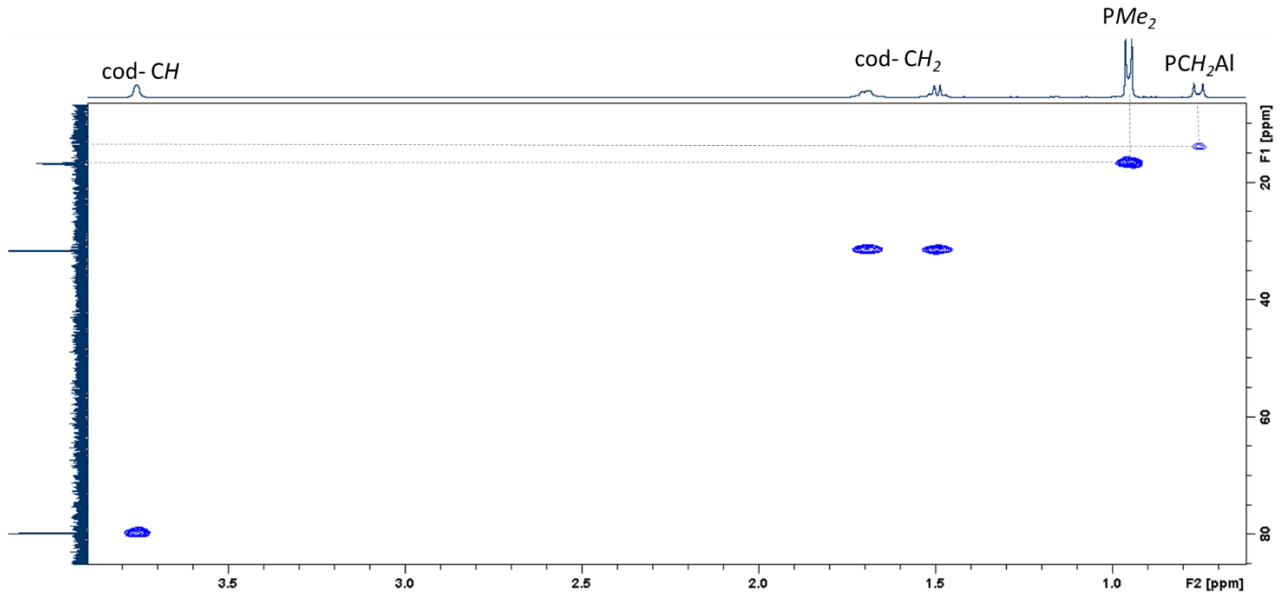

Figure S21. *2D HSQC HC NMR Spectrum of [{κ²P,P-Cl₂Al(CH₂PMe₂)₂}Ir(cod)] (**5**) in C₆D₆ (500, 125.8 MHz, 298K).*

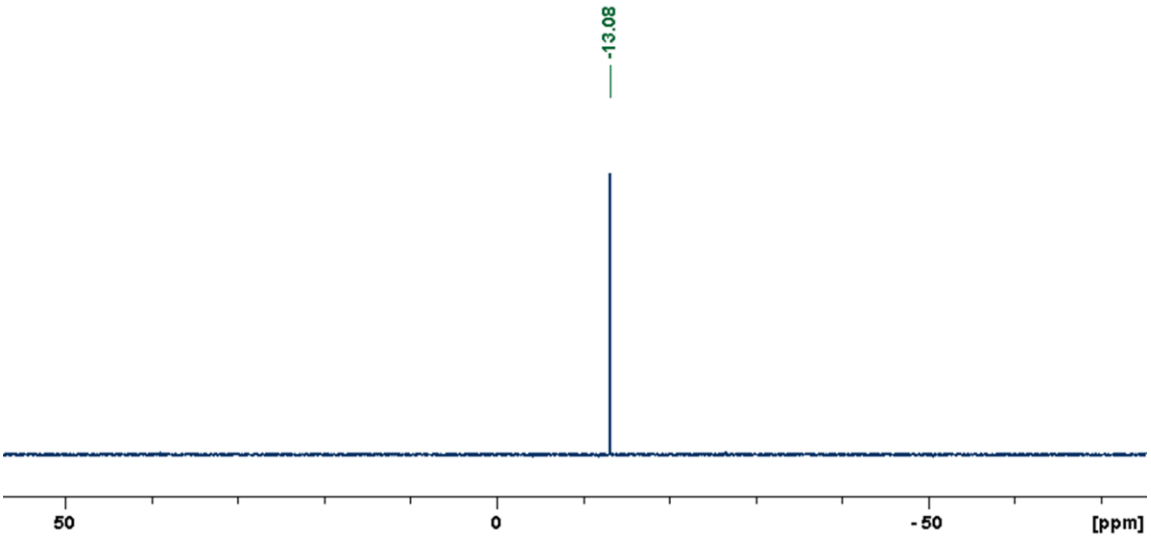

Figure S22. *$^{31}P\{^{1}H\}$ NMR Spectrum of [{κ²P,P-Cl₂Al(CH₂PMe₂)₂}Ir(cod)] (**5**) in C₆D₆ (202.5 MHz, 298K).*

NMR Spectra of [{κ²*P*,*P*-$Cl_2Al(CH_2PMe_2)_2$}Rh(cod)] (6)

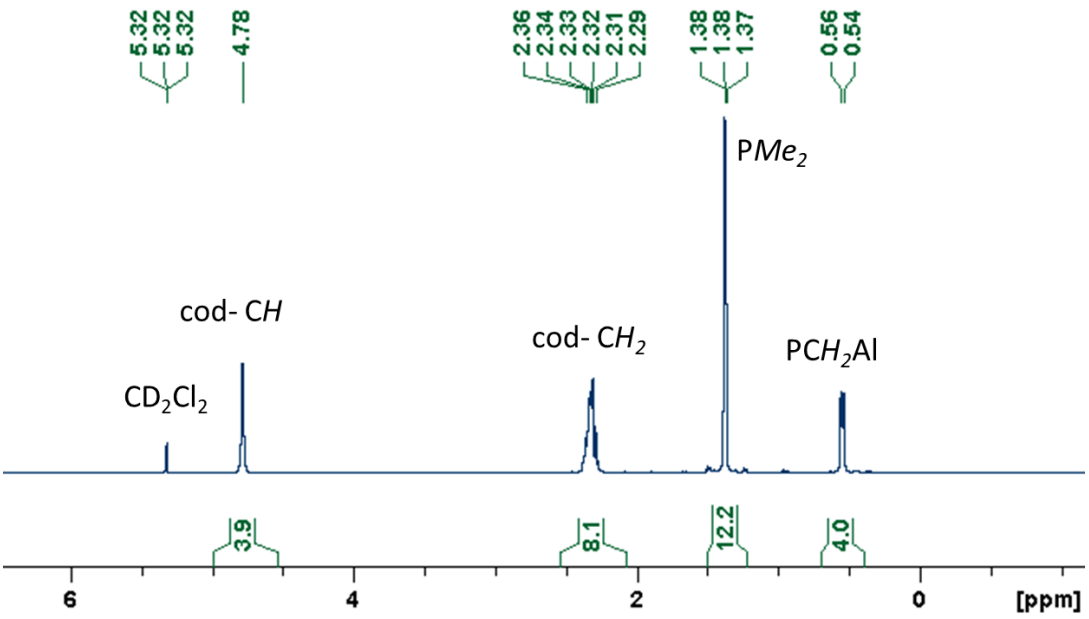

Figure S23. *^{1}H NMR Spectrum of [{κ²P,P-$Cl_2Al(CH_2PMe_2)_2$}Rh(cod)] (**6**) in CD_2Cl_2 (500 MHz, 298K).*

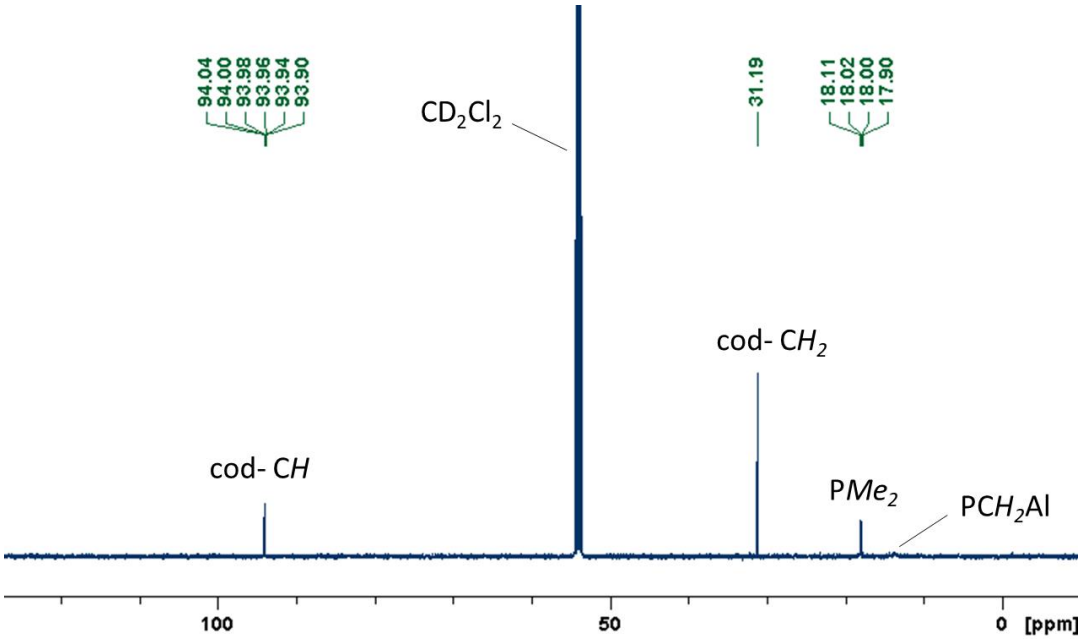

Figure S24. *$^{13}C\{^{1}H\}$ NMR Spectrum of [{κ²P,P-$Cl_2Al(CH_2PMe_2)_2$}Rh(cod)] (**6**) in CD_2Cl_2 (125.8 MHz, 298K).*

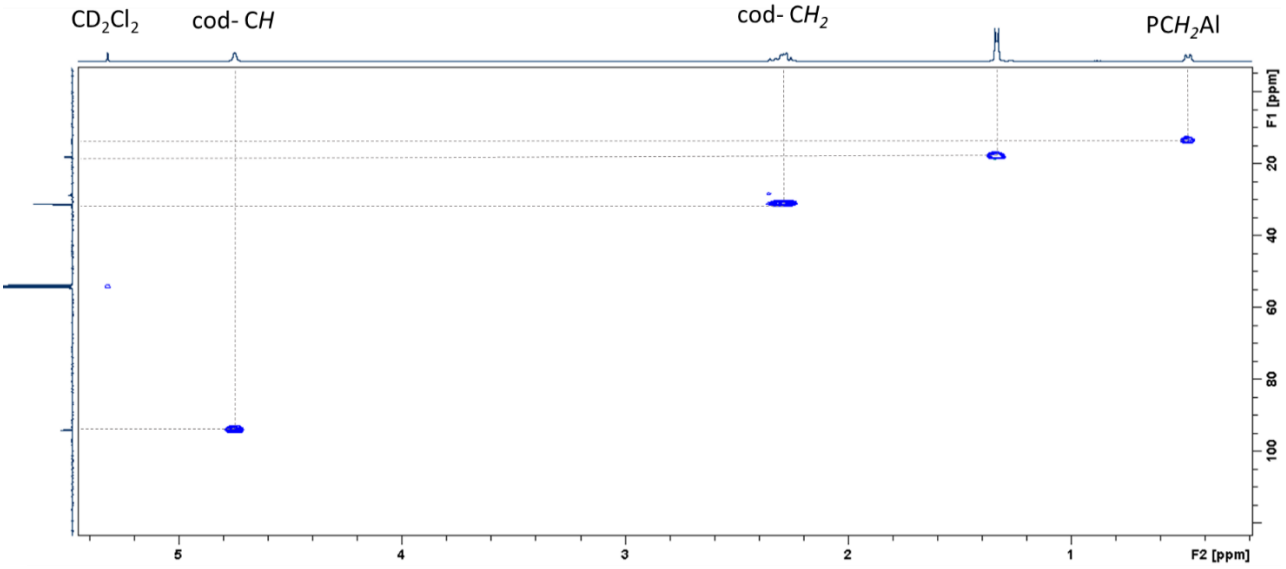

Figure S25. *2D HSQC H-C NMR Spectrum of [{κ²P,P-Cl₂Al(CH₂PMe₂)₂}Rh(cod)] (**6**) in CD₂Cl₂ (500, 125.8 MHz, 298K).*

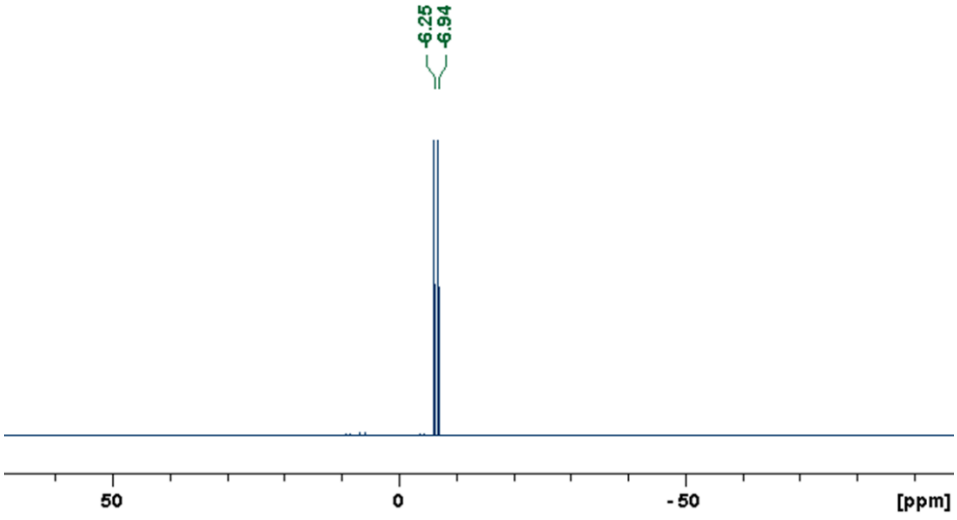

Figure S26. *$^{31}P\{^{1}H\}$ NMR Spectrum of [{κ²P,P-Cl₂Al(CH₂PMe₂)₂}Rh(cod)] (**6**) in CD₂Cl₂ (202.5 MHz, 298K).*

NMR Spectra of [(PtMe{μ-κ^1*P*:κ^2*P,P*-MeAl(CH$_2$PMe$_2$)$_3$})$_2$] (7)

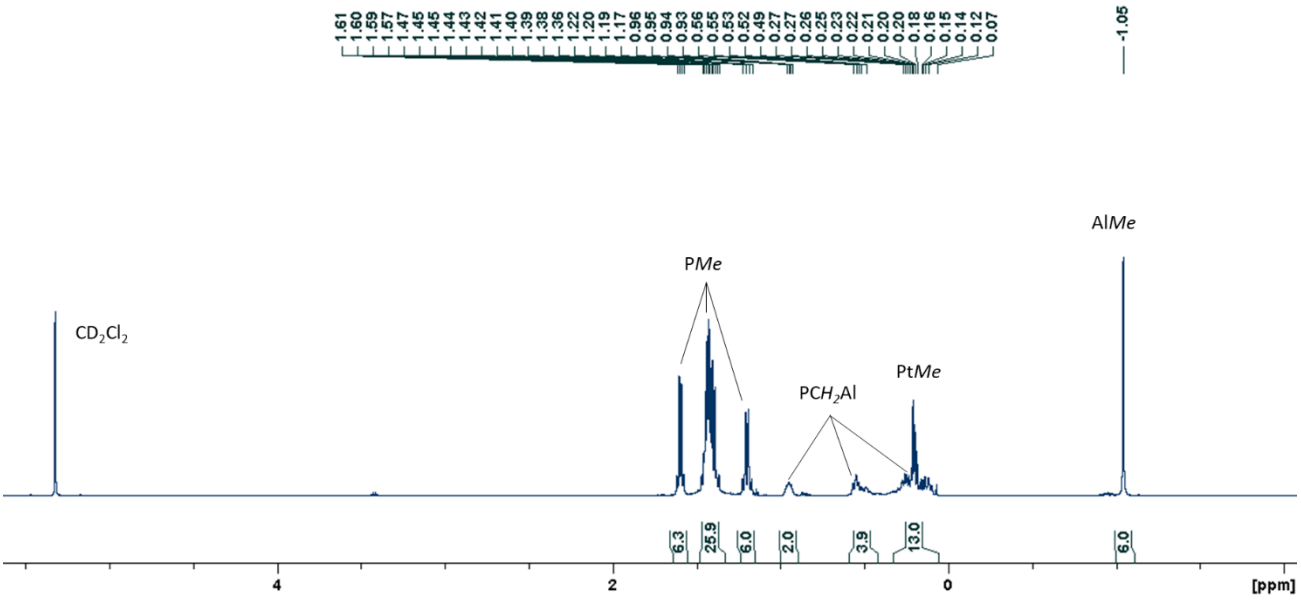

Figure S27. *^{1}H NMR Spectrum of [(PtMe{μ-κ^{1}P:κ^{2}P,P-MeAl(CH$_2$PMe$_2$)$_3$})$_2$] (**7**) in CD$_2$Cl$_2$ (600 MHz, 298K).*

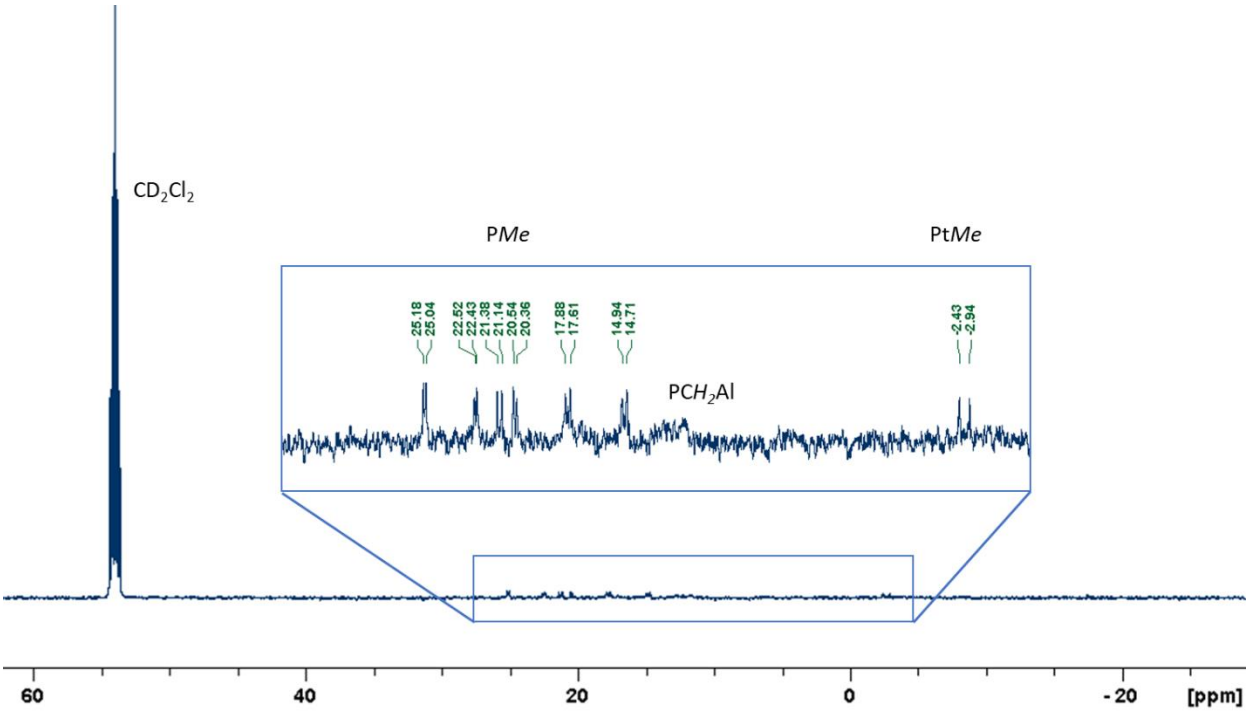

Figure S28. *^{13}C{^{1}H} NMR Spectrum of [(PtMe{μ-κ^{1}P:κ^{2}P,P-MeAl(CH$_2$PMe$_2$)$_3$})$_2$] (**7**) in CD$_2$Cl$_2$ (150.9 MHz, 298K; low signal to noise is due to poor solubility).*

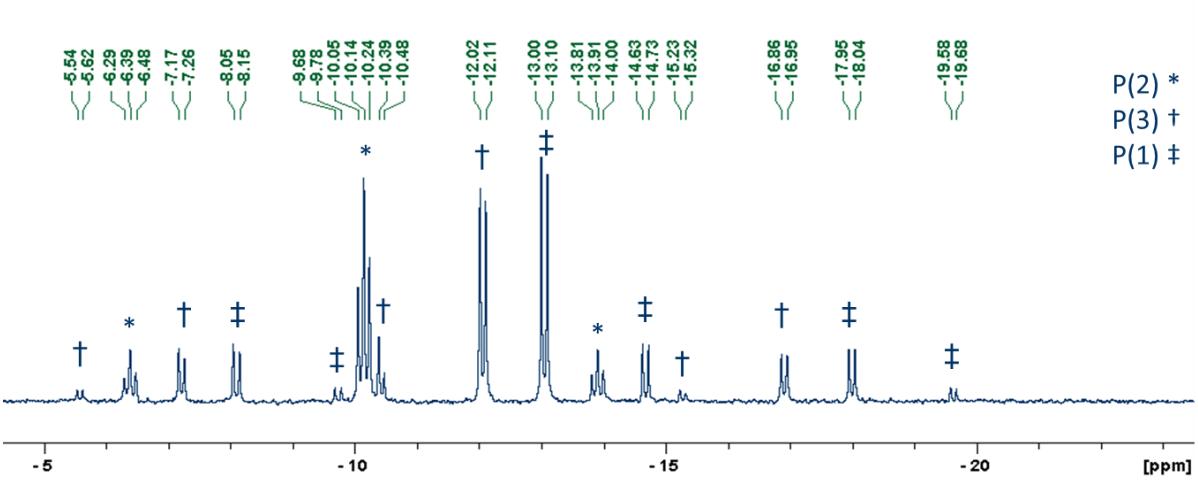

Figure S29. *$^{31}P\{^{1}H\}$ NMR Spectrum of [(PtMe{μ-κ^{1}P:κ^{2}P,P-MeAl(CH_2PMe_2)$_3$})$_2$] (**7**) in CD_2Cl_2 (242.9 MHz, 298K).*

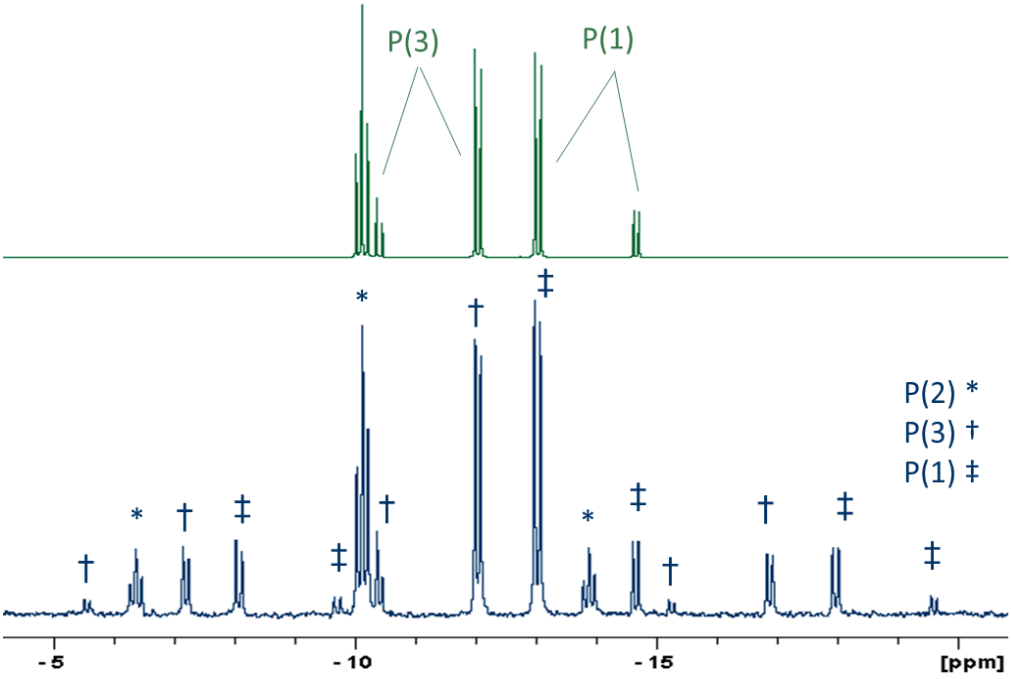

Figure S30. *$^{31}P\{^{1}H\}$ NMR Spectra of [(PtMe{μ-κ^{1}P:κ^{2}P,P-MeAl(CH_2PMe_2)$_3$})$_2$] (**7**) in C_6D_6 (242.9 MHz, 298K). The top spectrum is a simulation with the ^{195}Pt satellites excluded for clarity, and the experimental spectrum is at the bottom.*

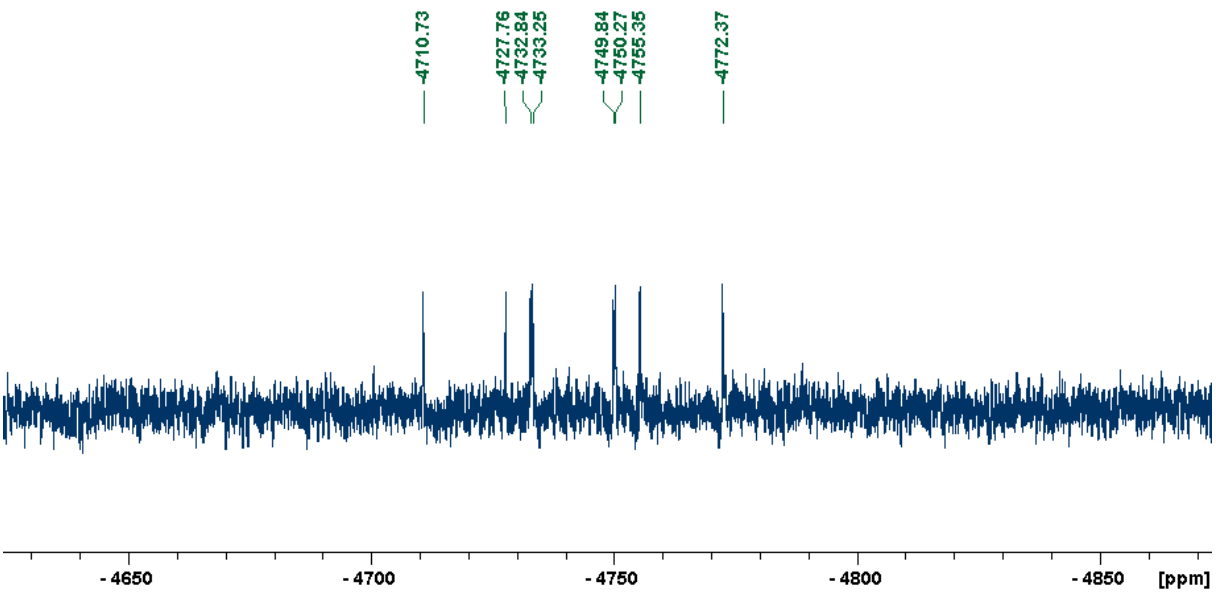

Figure S31. *^{195}Pt NMR Spectrum of [(PtMe{μ-κ^{1}P:κ^{2}P,P-MeAl(CH$_2$PMe$_2$)$_3$})$_2$] (**7**) in C$_6$D$_6$ (107.5 MHz, 298K).*

Table S1. Simulated ^{31}P chemical shifts $^2J_{P,P}$ coupling constants for [(PtMe{μ-κ^{1}P:κ^{2}P,P-MeAl(CH$_2$PMe$_2$)$_3$})$_2$] (**7**).

Atom	**δ (ppm)**	**$^2J_{P\text{-}P}$ 1 (Hz)**	**$^2J_{P\text{-}P}$ 2 (Hz)**	**$^2J_{P\text{-}P}$ 3 (Hz)**
P(2)	–10.14	-	22.6	22.6
P(3)	–11.53	22.6	-	397.9
P(1)	–13.59	22.6	397.9	-

NMR Spectra associated with reactions between $(Me_2PCH_2AlMe_2)_2$ and [AuCl(CO)] or $[PtCl_2(cod)]$

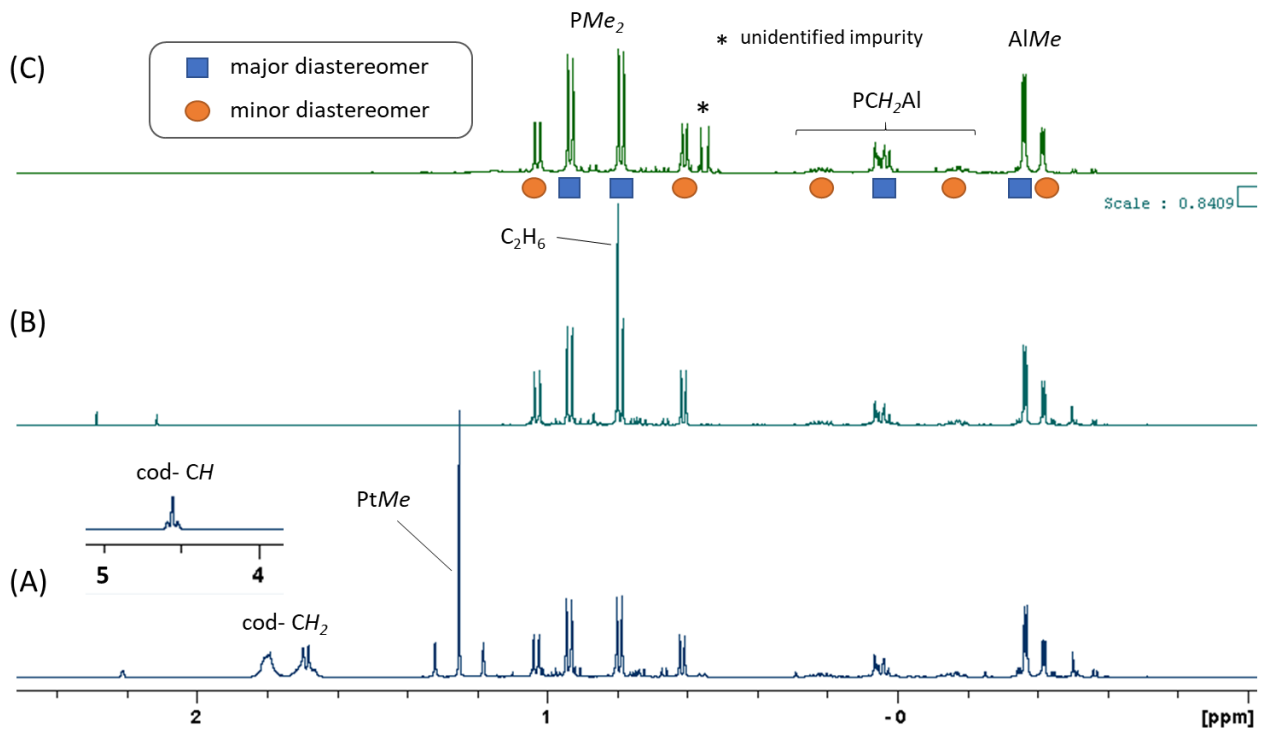

Figure S32. ^{1}H NMR Spectra for: (A) the 2:1 reaction between $(Me_2PCH_2AlMe_2)_2$ and $[PtCl_2(cod)]$ to afford $[PtMe_2(cod)]$ and $(Me_2PCH_2AlClMe)_2$, (B) the 1:1 reaction between $(Me_2PCH_2AlMe_2)_2$ and [AuCl(CO)] to afford Au(s), $(Me_2PCH_2AlClMe)_2$ and ethane, and (C) crystals of $(Me_2PCH_2AlClMe)_2$ obtained by recrystallization of the mother liquors from the 1:1 reaction between $(Me_2PCH_2AlMe_2)_2$ and [AuCl(CO)].

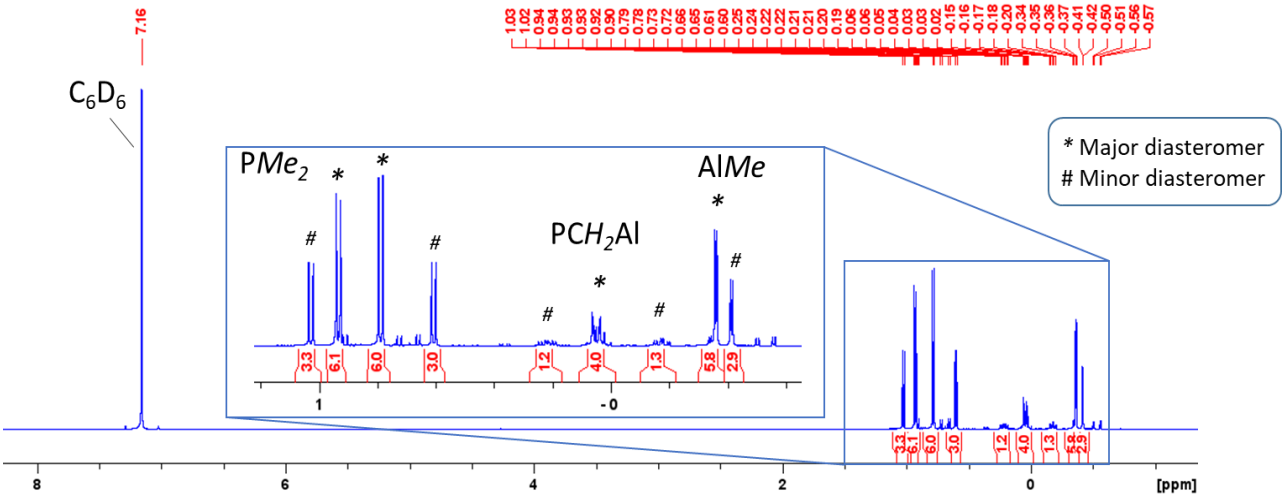

Figure S33. ^{1}H NMR Spectrum of $(Me_2PCH_2AlClMe)_2$ {from crystals obtained by recrystallization of the mother liquors from the 2:1 reaction of [AuCl(CO)] with $(Me_2PCH_2AlClMe)_2$} in C_6D_6 (600 MHz, 298K).

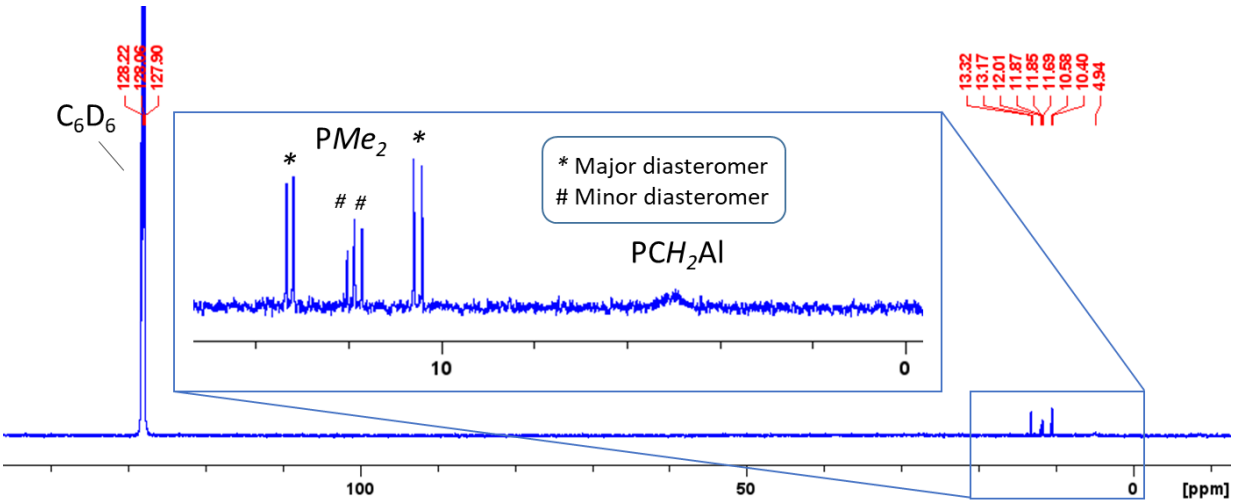

Figure S34. $^{13}C\{^{1}H\}$ NMR Spectrum of $(Me_2PCH_2AlClMe)_2$ {from crystals obtained by recrystallization of the mother liquors from the 2:1 reaction of [AuCl(CO)] with $(Me_2PCH_2AlClMe)_2$} in C_6D_6 (150.9 MHz, 298K). The broad P*C*H$_2$Al peak (confirmed by HSQC NMR) is for both diastereomers. The Al*Me* peaks were too broad to observe directly, but were located by HSQC NMR (see Figure S35).

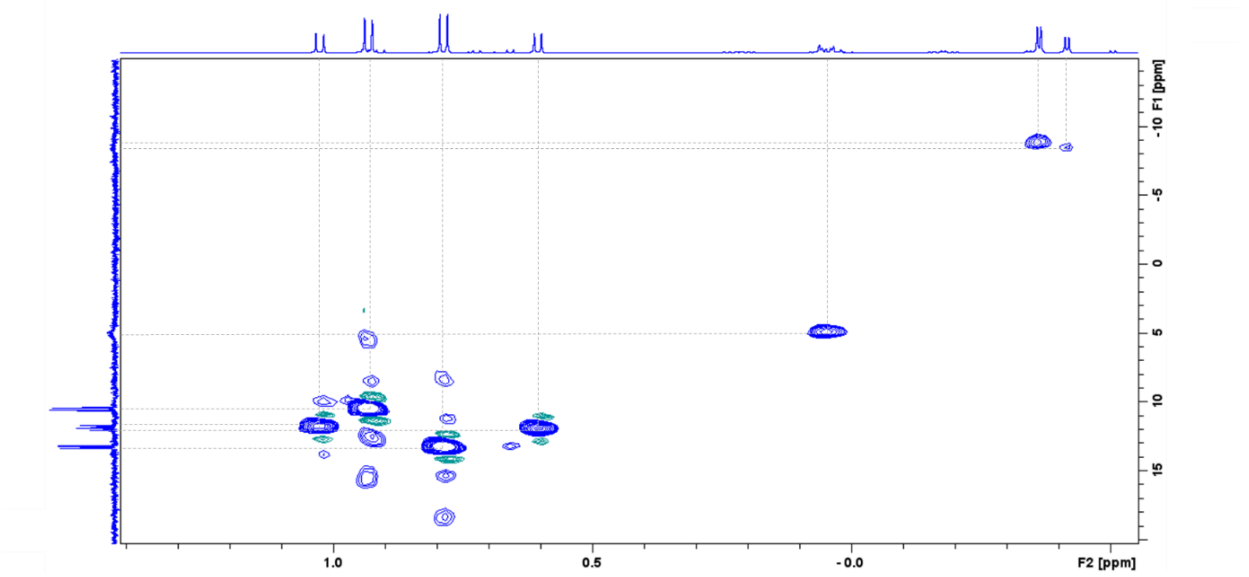

Figure S35. ^{1}H-^{13}C HSQC NMR Spectrum of $(Me_2PCH_2AlClMe)_2$ {from crystals obtained by recrystallization of the mother liquors from the 2:1 reaction of [AuCl(CO)] with $(Me_2PCH_2AlClMe)_2$} in C_6D_6 (600 MHz ^{1}H; 150.9 MHz ^{13}C; 298K).

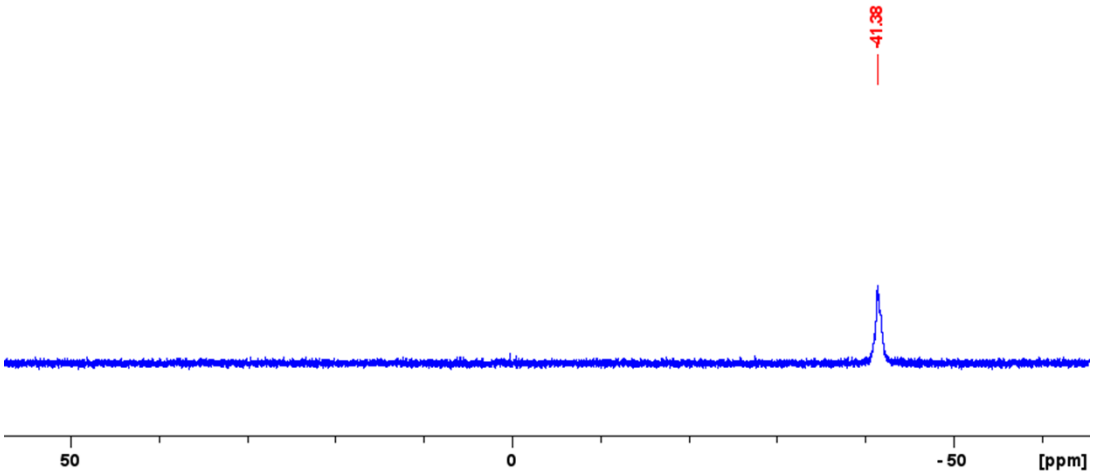

Figure S36. $^{31}P\{^{1}H\}$ NMR Spectrum of $(Me_2PCH_2AlClMe)_2$ {from crystals obtained by recrystallization of the mother liquors from the 2:1 reaction of [AuCl(CO)] with $(Me_2PCH_2AlClMe)_2$} in C_6D_6 (600 MHz, 298K).

NMR Spectra of the reaction of [Rh(cod)(μ-Cl)($Me_2PCH_2AlMe_2$)] (3) with THF to afford [{Rh(μ-CH_2PMe_2)(cod)}$_2$] (4)

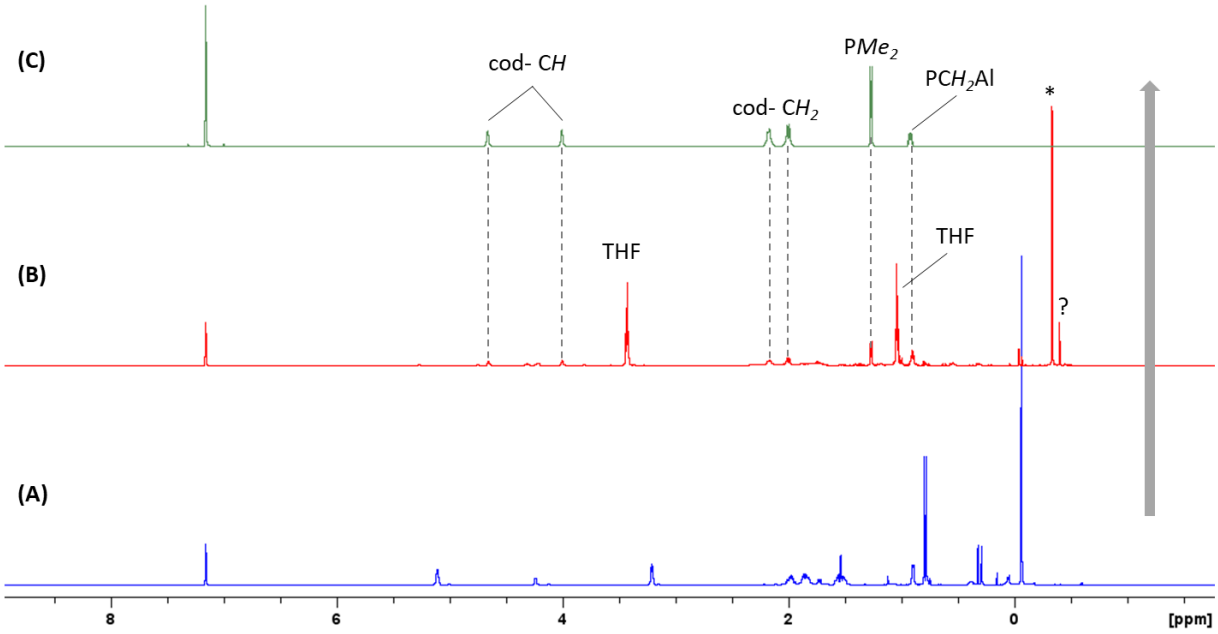

Figure S37. ^{1}H NMR spectra (C_6D_6, 500 MHz, 298 K) of: (A) the mixture of [Rh(cod)(μ-Cl)($Me_2PCH_2AlMe_2$)] (**3**; major product), [Rh(cod)(μ-Cl)($Me_2PCH_2AlClMe$)] (**3A**; minor product) and [{κ^2-ClMeAl(CH_2PMe_2)$_2$}Rh(cod)] (**2**; minor product) formed via the 1:1 reaction of ($Me_2PCH_2AlMe_2$)$_2$ with [{RhCl(cod)}$_2$], (B) the **3**/**3A**/**2** mixture from spectrum A after addition of excess THF, and (C) pure [{Rh(μ-CH_2PMe_2)(cod)}$_2$] (**4**) for comparison. The peak marked with an asterisk (at –0.33 ppm) is tentatively assigned as $Me_2AlCl(THF)_x$; see Figure 38.

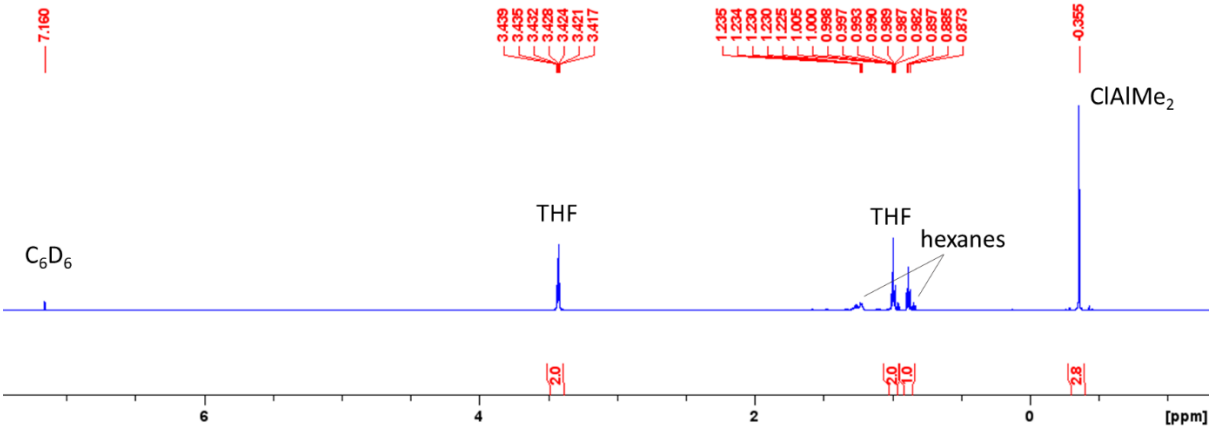

Figure S38. ^{1}H NMR spectra (C_6D_6, 500 MHz, 298 K) of $Me_2AlCl(THF)_x$. This solution was prepared by transferring a portion of a hexanes solution of Me_2AlCl (1.0 M; Sigma-Aldrich) into a J-young tube, application of vacuum to reduce the volume and concentrate the solution, addition of a drop of THF, and then addition of C_6D_6.

Powder X-Ray Diffraction Data

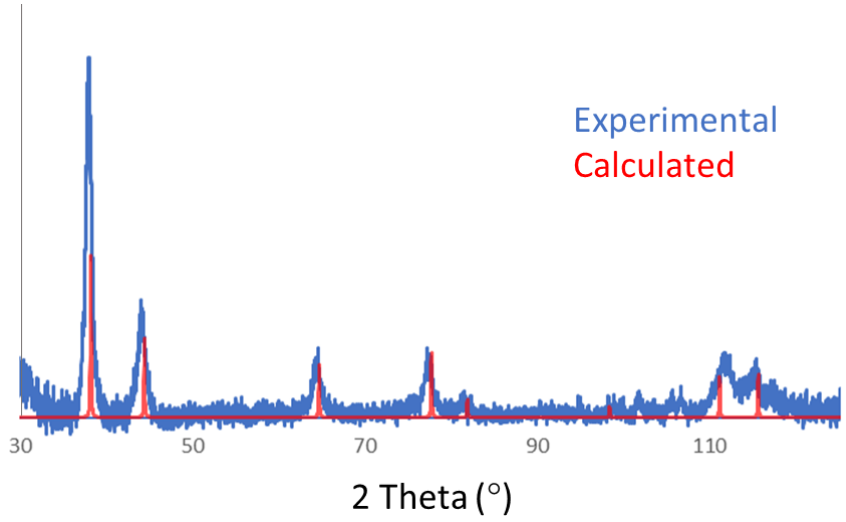

Figure S39. Powder X-ray diffractogram of the powder deposited from the 2:1 reaction between [AuCl(CO)] and $(Me_2PCH_2AlClMe)_2$} (298 K, Cu source, λ = 1.54056 Å). Red lines indicate the reference diffraction pattern corresponding to cubic gold, which was produced using Mercury Software with data retrieved from the Inorganic Crystal Structure Database (ICSD collection code: 163723)

Tables of Crystal Data and Crystal Structure Refinement

Table S2. *Crystal Data and Structure Refinement for [{κ^2P,P-(Me_3AlCl)MeAl(CH_2PMe_2)$_2$}Rh(cod)] (**1**).*

Table 1 Crystal data and structure refinement for RhcodPPAlMeClAlMe3.	
Identification code	RhcodPPAlMeClAlMe3
Empirical formula	$C_{18}H_{40}Al_2ClP_2Rh$
Formula weight	510.76
Temperature/K	100K
Crystal system	monoclinic
Space group	$P2_1/c$
a/Å	14.1403(16)
b/Å	9.6155(11)
c/Å	18.417(2)
α/°	90
β/°	92.833(2)
γ/°	90
Volume/Å^3	2501.0(5)
Z	4
ρ_{calc}g/cm^3	1.356
μ/mm^{-1}	0.988
F(000)	1064.0
Crystal size/mm^3	0.25 × 0.12 × 0.03
Radiation	MoKα (λ = 0.71073)
2Θ range for data collection/°	2.884 to 56.57
Index ranges	-18 ≤ h ≤ 18, -12 ≤ k ≤ 12, -24 ≤ l ≤ 24
Reflections collected	38203
Independent reflections	6201 [R_{int} = 0.0590, R_{sigma} = 0.0500]
Data/restraints/parameters	6201/204/241
Goodness-of-fit on F^2	1.027
Final R indexes [I>=2σ (I)]	R_1 = 0.0303, wR_2 = 0.0648
Final R indexes [all data]	R_1 = 0.0480, wR_2 = 0.0697
Largest diff. peak/hole / e Å^{-3}	0.56/-0.33

Table S3. *Crystal Data and Structure Refinement for [{κ^2P,P-ClMeAl(CH_2PMe_2)$_2$}Rh(cod)] (**2**).*

Identification code	RhcodPPAlMeCl
Empirical formula	$C_{15}H_{31}AlClP_2Rh$
Formula weight	438.68
Temperature/K	100.15
Crystal system	monoclinic
Space group	C2/c
a/Å	23.375(3)
b/Å	13.7736(18)
c/Å	11.9571(16)
α/°	90
β/°	92.852(2)
γ/°	90
Volume/Å^3	3844.9(9)
Z	8
ρ_{calc}g/cm^3	1.516
μ/mm^{-1}	1.229
F(000)	1808.0
Crystal size/mm^3	0.4 × 0.16 × 0.06
Radiation	MoKα (λ = 0.71073)
2Θ range for data collection/°	3.434 to 63.236
Index ranges	-34 ≤ h ≤ 34, -20 ≤ k ≤ 20, -17 ≤ l ≤ 17
Reflections collected	72957
Independent reflections	6425 [R_{int} = 0.0471, R_{sigma} = 0.0285]
Data/restraints/parameters	6425/2/194
Goodness-of-fit on F^2	1.082
Final R indexes [I>=2σ (I)]	R_1 = 0.0292, wR_2 = 0.0649
Final R indexes [all data]	R_1 = 0.0417, wR_2 = 0.0685
Largest diff. peak/hole / e Å^{-3}	0.96/-0.87

Table S4. *Crystal Data and Structure Refinement for [Rh(cod)(μ-Cl)($Me_2PCH_2AlMe_2$)] (**3**; 68 %) / [Rh(cod)(μ-Cl)($Me_2PCH_2AlClMe$)] (**3A**; 32 %).*

Identification code	RhcodClPAl
Empirical formula	$C_{25.36}H_{50.09}Al_2Cl_{2.64}P_2Rh_2$
Formula weight	770.36
Temperature/K	100.00(10)
Crystal system	triclinic
Space group	P-1
a/Å	11.2567(4)
b/Å	12.8343(5)
c/Å	13.1652(5)
α/°	71.297(2)
β/°	66.453(2)
γ/°	75.357(2)
Volume/Å³	1634.44(11)
Z	2
ρ_{calc}g/cm³	1.565
μ/mm⁻¹	1.391
F(000)	786.0
Crystal size/mm³	0.26 × 0.14 × 0.12
Radiation	MoKα (λ = 0.71073)
2Θ range for data collection/°	3.386 to 66.732
Index ranges	-17 ≤ h ≤ 17, -19 ≤ k ≤ 19, -20 ≤ l ≤ 20
Reflections collected	99188
Independent reflections	12623 [R_{int} = 0.0194, R_{sigma} = 0.0108]
Data/restraints/parameters	12623/0/327
Goodness-of-fit on F²	1.048
Final R indexes [I>=2σ (I)]	R_1 = 0.0175, wR_2 = 0.0468
Final R indexes [all data]	R_1 = 0.0196, wR_2 = 0.0476
Largest diff. peak/hole / e Å⁻³	0.95/-0.49

Table S5. *Crystal Data and Structure Refinement for [{Rh(μ-CH_2PMe_2)(cod)}$_2$] (**4**).*

Identification code	RhcodCH2PMe2
Empirical formula	$C_{22}H_{40}P_2Rh_2$
Formula weight	572.30
Temperature/K	100.0
Crystal system	monoclinic
Space group	I2/a
a/Å	18.1428(7)
b/Å	6.3491(3)
c/Å	19.3303(12)
α/°	90
β/°	93.2420(10)
γ/°	90
Volume/Å^3	2223.10(19)
Z	4
ρ_{calc}g/cm^3	1.710
μ/mm^{-1}	1.633
F(000)	1168.0
Crystal size/mm^3	0.18 × 0.1 × 0.06
Radiation	MoKα (λ = 0.71073)
2Θ range for data collection/°	4.22 to 67.448
Index ranges	-27 ≤ h ≤ 27, -9 ≤ k ≤ 9, -30 ≤ l ≤ 30
Reflections collected	47952
Independent reflections	4333 [R_{int} = 0.0349, R_{sigma} = 0.0227]
Data/restraints/parameters	4333/0/120
Goodness-of-fit on F^2	0.996
Final R indexes [I>=2σ (I)]	R_1 = 0.0190, wR_2 = 0.0452
Final R indexes [all data]	R_1 = 0.0256, wR_2 = 0.0461
Largest diff. peak/hole / e Å^{-3}	0.82/-0.53

Table S6. *Crystal Data and Structure Refinement for [{κ^2P,P-$Cl_2Al(CH_2PMe_2)_2$}Ir(cod)] (**5**).*

Identification code	IrcodPPAlCl2
Empirical formula	$C_{14}H_{28}AlCl_2IrP_2$
Formula weight	548.38
Temperature/K	100.00(10)
Crystal system	orthorhombic
Space group	Pbcn
a/Å	13.6878(3)
b/Å	11.8285(2)
c/Å	11.8398(2)
α/°	90
β/°	90
γ/°	90
Volume/Å^3	1916.94(6)
Z	4
ρ_{calc}g/cm^3	1.900
μ/mm^{-1}	7.446
F(000)	1064.0
Crystal size/mm^3	0.4 × 0.2 × 0.16
Radiation	MoKα (λ = 0.71073)
2Θ range for data collection/°	4.552 to 80.586
Index ranges	$-24 \le h \le 24$, $-21 \le k \le 21$, $-21 \le l \le 21$
Reflections collected	152846
Independent reflections	6060 [R_{int} = 0.0341, R_{sigma} = 0.0108]
Data/restraints/parameters	6060/0/94
Goodness-of-fit on F^2	1.147
Final R indexes [I>=2σ (I)]	R_1 = 0.0199, wR_2 = 0.0445
Final R indexes [all data]	R_1 = 0.0277, wR_2 = 0.0483
Largest diff. peak/hole / e Å^{-3}	3.12/-1.28

Table S7. *Crystal Data and Structure Refinement for [{κ^2P,P-$Cl_2Al(CH_2PMe_2)_2$}Rh(cod)] (**6**).*

Identification code	RhcodPPAlCl2
Empirical formula	$C_{14}H_{28}AlCl_2P_2Rh$
Formula weight	459.09
Temperature/K	100.0
Crystal system	orthorhombic
Space group	Pbcn
a/Å	13.6821(3)
b/Å	11.8577(3)
c/Å	11.8639(3)
α/°	90
β/°	90
γ/°	90
Volume/Å³	1924.78(8)
Z	4
ρ_{calc}g/cm³	1.584
μ/mm⁻¹	1.366
F(000)	936.0
Crystal size/mm³	0.36 × 0.28 × 0.22
Radiation	MoKα (λ = 0.71073)
2Θ range for data collection/°	4.546 to 76.138
Index ranges	-23 ≤ h ≤ 23, -20 ≤ k ≤ 20, -20 ≤ l ≤ 20
Reflections collected	64958
Independent reflections	5194 [R_{int} = 0.0200, R_{sigma} = 0.0094]
Data/restraints/parameters	5194/0/118
Goodness-of-fit on F²	1.104
Final R indexes [I>=2σ (I)]	R_1 = 0.0179, wR_2 = 0.0479
Final R indexes [all data]	R_1 = 0.0210, wR_2 = 0.0495
Largest diff. peak/hole / e Å⁻³	1.04/-0.34

Table S8. *Crystal Data and Structure Refinement for [(PtMe{μ-κ^1P:κ^2P,P-MeAl(CH_2PMe_2)$_3$})$_2$] (**7**).*

Identification code	PtPPPAlMe
Empirical formula	$C_{22}H_{60}Al_2P_6Pt_2$
Formula weight	954.66
Temperature/K	100.0
Crystal system	triclinic
Space group	P-1
a/Å	9.4084(3)
b/Å	9.6824(3)
c/Å	11.1418(4)
α/°	103.209(2)
β/°	107.622(2)
γ/°	105.478(2)
Volume/Å^3	877.82(5)
Z	1
ρ_{calc}g/cm^3	1.806
μ/mm^{-1}	8.294
F(000)	464.0
Crystal size/mm^3	0.22 × 0.2 × 0.18
Radiation	MoKα (λ = 0.71073)
2Θ range for data collection/°	4.636 to 77.178
Index ranges	-16 ≤ h ≤ 16, -16 ≤ k ≤ 16, -19 ≤ l ≤ 19
Reflections collected	85463
Independent reflections	9849 [R_{int} = 0.0367, R_{sigma} = 0.0207]
Data/restraints/parameters	9849/0/153
Goodness-of-fit on F^2	1.066
Final R indexes [I>=2σ (I)]	R_1 = 0.0173, wR_2 = 0.0367
Final R indexes [all data]	R_1 = 0.0204, wR_2 = 0.0375
Largest diff. peak/hole / e Å^{-3}	1.71/-0.73

Table S9. Crystal Data and Structure Refinement for *meso*-$(Me_2PCH_2AlClMe)_2$.

Identification code	PAlMeCl
Empirical formula	$C_8H_{22}Al_2Cl_2P_2$
Formula weight	305.05
Temperature/K	100.00(10)
Crystal system	triclinic
Space group	P-1
a/Å	6.5589(2)
b/Å	7.5892(2)
c/Å	9.2977(2)
α/°	76.9990(10)
β/°	70.5430(10)
γ/°	66.6410(10)
Volume/Å³	398.300(19)
Z	1
ρ_{calcg}/cm³	1.272
μ/mm⁻¹	0.688
F(000)	160.0
Crystal size/mm³	0.15 × 0.15 × 0.08
Radiation	MoKα (λ = 0.71073)
2Θ range for data collection/°	5.882 to 65.48
Index ranges	-9 ≤ h ≤ 9, -11 ≤ k ≤ 11, 0 ≤ l ≤ 14
Reflections collected	8302
Independent reflections	8302 [R_{int} = ?, R_{sigma} = 0.0255]
Data/restraints/parameters	8302/0/69
Goodness-of-fit on F²	1.061
Final R indexes [I>=2σ (I)]	R_1 = 0.0318, wR_2 = 0.0783
Final R indexes [all data]	R_1 = 0.0407, wR_2 = 0.0822
Largest diff. peak/hole / e Å⁻³	0.55/-0.36